



Published in final edited form as:

*Doc Ophthalmol.* 2010 February ; 120(1): 25–39. doi:10.1007/s10633-009-9181-x.

## The Effects of Oxygen Stresses on the Development of Features of Severe Retinopathy of Prematurity

M. Elizabeth Hartnett, MD

Professor of Ophthalmology, Department of Ophthalmology, University of North Carolina, 130 Mason Farm Road, CB #7040, Chapel Hill, NC 27599-7040

### Abstract

**Purpose**—To describe the effects of oxygen fluctuations and supplemental oxygen (SO), stresses relevant to preterm infants today, on growth factor expression and activation of signaling pathways associated with intravitreal neovascularization and avascular retina, features of severe retinopathy of prematurity (ROP).

**Methods**—Review of articles using 50/10 oxygen-induced retinopathy (OIR) and 50/10 OIR+SO models

**Results**—Repeated fluctuations in oxygen increased retinal VEGF even while avascular retina persisted and prior to the development of intravitreal neovascularization. Hypoxia increased VEGF<sub>120</sub> expression whereas repeated fluctuations in oxygen increased VEGF<sub>164</sub>. Neutralizing VEGF bioactivity significantly reduced intravitreal neovascularization and arteriolar tortuosity without interfering with ongoing retinal vascularization. Repeated oxygen fluctuations led to retinal hypoxia and increased reactive oxygen species (ROS). Inhibiting ROS with NADPH oxidase inhibitor, apocynin, reduced avascular retina by interfering with apoptosis. Supplemental oxygen reduced retinal VEGF concentration and exacerbated NADPH oxidase activation to contribute to intravitreal neovascularization through activation of JAK/STAT pathway.

**Conclusion**—Oxygen stresses relevant to those experienced by preterm infants today trigger signaling of different pathways to cause avascular retina and intravitreal neovascularization.

### Keywords

retinopathy of prematurity; intravitreal neovascularization; stage 3 ROP; zone; supplemental oxygen; fluctuations in oxygen; avascular retina; vascular endothelial growth factor; JAK/STAT; NADPH oxidase

### Introduction

Our laboratory has been interested in the question why blood vessel growth proceeds into the vitreous, rather than into the retina, in retinopathy of prematurity (ROP). We use oxygen stresses similar to those experienced by preterm infants who develop severe ROP in modern-day. We have studied the effects of oxygen stresses on retinal vascular development, growth factor expression, and signaling pathways involving mostly angiogenesis. We use the rat model of repeated fluctuations in oxygen developed by John Penn (50/10 OIR model), because this model has similarities to the oxygen stresses that preterm infants experience in modern-day neonatal intensive care units and develops an appearance similar to stage 3 ROP

with intravitreal neovascularization at the junction of vascular and avascular retina (Figure 1). We also study the effect of supplemental oxygen (SO) using the 50/10 OIR+SO model<sup>1</sup>. By understanding the causes of abnormal blood vessel growth, we strive to determine methods to not only inhibit intravitreal blood vessel growth, but also to facilitate intraretinal vascularization of the previously avascular retina (Figure 2).

## Significance

Blood vessel growth into the vitreous precedes the formation of complex traction retinal detachments in ROP that can lead to complete blindness in preterm infants. Even with successful retinal reattachment through surgery, vision is often poor<sup>2</sup>. Therapies to reduce abnormal blood vessel growth using ablation to the peripheral avascular retina with cryotherapy<sup>3</sup> or laser<sup>4</sup> have led to significantly improved visual outcomes.

## Features Important in Severe ROP: Avascular Retina and Intravitreal Neovascularization

Multicenter clinical trials have shown that preterm infant eyes with the largest peripheral retinal avascular zones have the worst outcomes from ROP<sup>5,6</sup>. The avascular, hypoxic retina is believed to be a source of angiogenic factors that cause pathologic intravitreal neovascularization in some models of ROP<sup>7,8</sup>. However, what causes avascular retina initially remains largely unknown. ROP was first described in the 1940's<sup>9</sup> as retrolental fibroplasia for the appearance of the worst stage (now called stage 5 ROP indicating total retinal detachment with a retrolental fibrovascular membrane). At that time, there was inadequate technology to carefully monitor oxygen levels in premature infants in neonatal intensive care units. Vaso-obliteration of newly formed and fragile retinal vessels from high oxygen likely played a role in early forms of ROP. However, with improved oxygen monitoring and recognition of earlier stages of ROP, delayed retinal vascularization has also been recognized as an important contributor to avascular retina. Delayed retinal vascular development in *bcl2*<sup>-/-</sup> mice that have a defect in protection against apoptosis, supports the thinking that increased apoptosis of endothelial cells or their precursors may contribute to avascular retina<sup>10</sup>. Other data support apoptosis, or programmed cell death, as a mechanism. Protection of newly formed capillaries from hyperoxia-induced endothelial death occurs by giving growth factors like insulin-like growth factor-1 (IGF-1) or a binding protein to IGF-1, placental growth factor-1, VEGF<sup>11-14</sup>, or nutritional supplements, including amino acids (arginyl-glutamine) or omega 3 fatty acids<sup>15,16</sup> prior to the hyperoxic insult. We reported that presumed reactive oxygen species released from activated nicotinamide adenine dinucleotide (phosphate) (NADPH oxidase) after repeated oxygen fluctuations contributed to the avascular retina through apoptosis<sup>17</sup>. Thus, the area of avascular retina is associated with the severity of human ROP, and apoptosis may contribute to the avascular retinal area.

ROP may differ from other retinovascular diseases associated with avascular retina, such as proliferative diabetic retinopathy. In ROP, regression of disease often is associated with intraretinal vascularization into the previously avascular retina. The avascular retina thus appears able to support intraretinal vascularization in ROP, whereas in diabetic retinopathy, this appears less often.

## Fluctuations in Oxygen: Effects on Retinal Vascular Development and Modern-day ROP

When ROP was first described in the 1940's, it was likely a result of high unregulated oxygen at birth<sup>18-20</sup>. Several animal models were developed to study the causes of the disease<sup>19,21</sup>. These models exposed newborn animals to very high constant oxygen that

caused vaso-obliteration of newly formed susceptible capillaries. Then following room air exposure, intravitreal endothelial budding into the vitreous occurred. The results of this early research led to improvements in oxygen monitoring and the avoidance of high, unregulated oxygen at birth. ROP virtually disappeared. However, as infants of younger gestational ages and smaller birth weights survived, ROP re-emerged. Now, rather than high inspired oxygen at birth, it is recognized that fluctuations in transcutaneous oxygen levels are also important risks for severe ROP<sup>22–27</sup>. (The fluctuations in oxygen are proposed to cause fluctuations in retinal oxygenation and be secondary to changes in both inspired and blood oxygen concentration resulting from episodes of bradycardia and apnea of prematurity.)

Rats raised from birth in fluctuations of oxygen rather than room air developed areas of peripheral avascular retina (John Penn performed this work and developed the rat models for ROP. Penn's work is discussed elsewhere in this issue). Further, certain extremes and ranges in oxygen levels led to avascular retina and intravitreal neovascularization at the junctions of vascular and avascular retina<sup>28</sup>. Pups cycled between 45% and 12.5% inspired oxygen every 24 hours, rather than 40% and 15%, had more severe intravitreal neovascularization and greater avascular retina. When oxygen was cycled between 50% and 10% every 24 hours (50/10 OIR model), the pups develop an appearance similar to that of infants with stage 3 ROP (compare Figure 1 and Figure 3). In the human preterm infant that develops severe ROP, Cunningham and McCollm found that transcutaneous oxygen levels fluctuated on a minute to minute basis in preterm infants who developed severe ROP<sup>22</sup>. The extremes in oxygen levels were similar to the arterial oxygen concentrations that occurred in rats in the “Penn 50/10” OIR model. Furthermore, when these oxygen levels were recapitulated in newborn (not premature) rats with minute-to-minute fluctuations, peripheral avascular retina occurred, but to a lesser degree than when fluctuations occurred every 24 hours<sup>29</sup>. Most other models of oxygen induced retinopathy, including the mouse model<sup>30</sup>, use high constant inspired oxygen that causes high blood oxygen concentration<sup>31</sup> to induce central capillary obliteration rather than peripheral avascular retina (see lectin-stained retinal flat mount of mouse model, Figure 4). Therefore, besides high oxygen at the time of birth, it appears that in ROP of modern-day, fluctuations in oxygen play a role in the development of pathologic features of severe ROP, and there is laboratory evidence supporting oxygen fluctuations with the clinical findings.

## Supplemental Oxygen in Modern-day ROP

Animal studies using the kitten model of high hyperoxia<sup>32</sup> or the mouse model<sup>33</sup> found that animals recovered in supplemental oxygen rather than in room air had less severe retinopathy. Based on this, a multicenter clinical trial was set up to determine if supplemental oxygen vs. conventional treatment in infants who developed prethreshold ROP would reduce the occurrence of threshold ROP (severe ROP in which the risk of retinal detachment - stage 5 ROP - approached 50%<sup>3</sup>). Although the Supplemental Therapeutic Oxygen for Prethreshold Retinopathy of Prematurity (STOP-ROP) study found no adverse effect from supplemental oxygen and perhaps a benefit in a subgroup<sup>34</sup>, several studies now report that severe ROP is more common in preterm infants who have had high oxygen saturations at some points in their management in neonatal intensive care units<sup>35,36</sup>.

## Methods

### 50/10 OIR model and 50/10 OIR + SO model

All animal studies complied with the University of North Carolina's Institute for Laboratory Animal Research (Guide for the Care and Use of Laboratory Animals) and the ARVO Statement for the Use of Animals in Ophthalmic and Visual Research.

In the 50/10 OIR model, pups within 4 hours of birth were placed with their moms into an oxygen-regulated environment (Oxycycler, Biospherix, New York, NY) in which they were exposed to 50% oxygen for 24 hours followed by 10% oxygen for 24 hours<sup>37</sup>. This cycle was repeated 7 times until day 14 (Figure 5). Oxygen levels were monitored daily and recalibrated as needed. Carbon dioxide in the cage was also monitored daily and flushed from the system by maintaining sufficient gas-flow and by adding soda lime. Pup number per litter was maintained between 12 and 14. At postnatal day (p)12, retinal arteriolar tortuosity developed<sup>38,39</sup> and at p14, peripheral retinal avascular retina was ~30% of total retinal area similar to that seen zone II human ROP (Table 1). At day 14, pups were placed into room air for 4 days (50/10 OIR model) or into 28% oxygen (50/10 OIR + SO model, Figure 5). At p18 to p20, intravitreal neovascularization occurred at the junction of vascular and avascular retina similar to stage 3 ROP (Figure 3 and Figure 4)<sup>40</sup>. These features are reproducible and can be quantified and compared (Figure 6).

Specific methods are discussed in papers referenced below. In general, pathologic features of severe ROP were avascular retina, retinal tortuosity, and intravitreal neovascularization. Avascular retina was measured using ImageTool (v.3, University of Texas, TX) and the avascular/total retinal area determined from lectin stained retinal flat mounts. Vessel tortuosity was analyzed by tracing the vessel extent using ROptool (version 1.1, from the University of North Carolina Computer-Aided Diagnosis and Display Laboratory<sup>41</sup>). Intravitreal neovascularization was analyzed by counting the number of clock hours involved or summing areas of neovascularization. Retinal sections were made from cryopreserved whole eyes (except for cornea, lens and vitreous) and co-labeled for cell markers and proteins. mRNA and protein were determined from whole fresh retinas minus the ora serrata. Systemic (intraperitoneal injections) or intravitreal injections were performed to test the effects of agents on features and signaling pathways.

## Studies and Results

### Effects of Oxygen Fluctuations on Angiogenic Factor, VEGF, and Inhibitory Factor, PEDF

Vascular endothelial growth factor (VEGF) is an essential growth factor in retinal vascular development<sup>42,43</sup>. It is also important as a survival factor for newly developed vessels and for adult vascular beds<sup>44,45</sup>. However, it can be a major factor involved in pathologic angiogenesis in a number of diseases in animal models and humans, including those associated with intravitreal neovascularization<sup>46,47</sup>. A knockout of even one allele of VEGF or of receptor 1 [VEGFR1 (flt-1)] or receptor 2 [VEGFR2 (KDR, Flk)], is lethal. Therefore, the effects of VEGF can be studied by blocking the biological actions of VEGF through inhibitors or antibodies. Pigment epithelial derived factor (PEDF) is also important in retinal vascular development<sup>48</sup>, and has been shown to be a potent anti-angiogenic factor with ability to inhibit VEGF induced angiogenesis<sup>48-50,51</sup>. Since these two factors are important in both retinal vascular development and pathologic angiogenesis, we studied the role of oxygen stresses on the regulation of VEGF and PEDF.

In several animal models using hyperoxia induced vaso-obliteration, investigators found that retinal VEGF expression was reduced during periods of high constant oxygen<sup>51,52</sup> and increased during relative hypoxia<sup>42,43</sup> upon return to room air<sup>30</sup> (Figure 4). The increase in VEGF expression was also associated with angiogenesis during normal vascular development with physiologic hypoxia<sup>42,43</sup>. However, less has been studied on the effects of oxygen fluctuations on the expression of VEGF over time in development using models that replicate the oxygen stresses experienced by modern-day preterm infants who develop ROP. We studied the effects of different numbers of oxygen fluctuations on the percent avascular retina and on the expression of VEGF and of its mRNA isoforms, caused by alternative splicing of the parent mRNA. The isoforms have been shown to have different biological

activities<sup>53–58</sup>. Compared to room air, pups raised in the 50/10 OIR model had increased avascular/total retinal area at all time points tested [Table 1].

VEGF has several angiogenic isoforms of the parent mRNA. There are at least 5 pro-angiogenic VEGF mRNA isoforms in humans and 3 in mice that develop from alternative splicing of the parent gene. The most studied are (with mouse/rat analogs in parentheses) VEGF<sub>189</sub> (VEGF<sub>188</sub>), VEGF<sub>121</sub> (VEGF<sub>120</sub>), and VEGF<sub>165</sub> (VEGF<sub>164</sub>)<sup>59</sup>. The isoforms have different biologic functions based on differences in heparin binding, which determines the gradient generated<sup>53–58</sup>. VEGF<sub>164/165</sub> is the most prevalent and also increases leukostasis, endothelial apoptosis, and avascular retina through inflammatory mechanisms in some models<sup>54</sup>. VEGF<sub>120/121</sub> is soluble and VEGF<sub>188/189</sub> is believed involved in endothelial adhesion and migration<sup>60,61</sup>. Since VEGF is important in development as well as in pathologic angiogenesis, we wished to understand whether it was the expression of certain isoforms that was dysregulated under oxygen stress. We first determined the effect of hypoxia versus repeated oxygen fluctuations (i.e., the 50/10 OIR model) on the expression of isoforms of the parent VEGF mRNA<sup>62</sup>. A single episode of 10% oxygen at p7 or p14 caused a significantly increased fold change in VEGF<sub>120</sub>, the soluble isoform, compared to room air, but not the “pathologic” VEGF<sub>164</sub>, as determined by relative quantitative PCR. On the other hand, repeated fluctuations in oxygen caused a greater fold difference in VEGF<sub>164</sub> mRNA compared to a single episode of 10% oxygen [Figure 7]. Furthermore, with ELISA testing, which would measure protein of all isoforms but represent mainly the most prevalent isoform (VEGF<sub>164</sub>), there was greater fold increase in VEGF protein following repeated fluctuations in oxygen rather than after one cycle between 50% and 10% oxygen (both time points were immediately following hypoxia). We did not find a significant difference in fold change in mRNA of PEDF between room air- and 50/10 OIR-exposed rat pups at several time points. However, PEDF expression was greater at early postnatal day ages than at later ones in the 50/10 model compared to room air<sup>62</sup>.

We extended these studies to determine whether VEGF expression was increased after return to room air and preceding the development of intravitreal neovascularization. This would be analogous to other models of hyperoxia induced vaso-obliteration and angiogenesis, in which VEGF expression was reduced during vaso-obliteration from hyperoxia and increased during angiogenesis upon return to room air. Using ELISA, we measured VEGF protein in retinas from rats raised in room air or the 50/10 OIR model. However, we found that VEGF was significantly greater than room air at p12 and p14 while avascular retina was present in the 50/10 OIR model prior to return to room air (Figure 8).

From these studies, we learned that VEGF<sub>164</sub> was the most prevalent isoform both in room air and the 50/10 OIR model. VEGF<sub>164</sub> expression was increased by repeated fluctuations in oxygen whereas VEGF<sub>120</sub> expression was increased by hypoxia<sup>62</sup>. Although VEGF expression was increased by repeated oxygen fluctuations compared to that in room air, retinal vascular development was delayed and intravitreal neovascularization occurred.

Gerhardt et al<sup>63</sup> injected very high concentrations of VEGF into the vitreous and found that endothelial tip cells pointed filopodia (believed important in providing guidance cues for migrating endothelial cells) toward the vitreous. These observations led us to the hypothesis that the chemotactic force of vitreous VEGF would attract endothelial cells to grow away from the retina and into the vitreous in diseases with intravitreal neovascularization. We sought evidence for this hypothesis by measuring VEGF protein in the vitreous and retina of animals in the 50/10 OIR model. Compared to room air, we found at least 10-fold greater retinal VEGF at p12, p14, and p18 in the 50/10 OIR model<sup>64</sup> (Figure 8; Table 2). However, in the 50/10 OIR model, the retinal concentration of VEGF at p18 was at least 10 fold greater than that in the vitreous (Table 3)<sup>64</sup>, and this finding argued against the hypothesis

that vitreous VEGF concentration would provide a chemotactic gradient for migrating endothelial cells.

### Effects of VEGF Inhibition on Avascular Retina and Intravitreal Neovascularization in the 50/10 OIR Model

We then wished to determine if inhibiting the bioactivity of VEGF using a neutralizing antibody to VEGF would affect retinal vascular development or intravitreal neovascularization. Based on findings that retinal VEGF was greatest at p14 in the 50/10 OIR model<sup>64</sup>, we chose to inject a neutralizing antibody made against VEGF<sub>164</sub> into the vitreous of rats in the 50/10 OIR model. Compared to a nonimmune IgG control, 50 ng of a neutralizing antibody to VEGF significantly reduced clock hours of intravitreal neovascularization (50% reduction) without interfering with retinal vascular development determined as avascular/total retinal area (Figure 9). This dose reduced phosphorylated VEGF receptor 2 labeling in retinal cryosections but not phosphorylated VEGF receptor 1<sup>64</sup>. The evidence supported that inhibition of VEGF signaling through VEGFR2 appeared to reduce intravitreal neovascularization without further interfering with retinal vascular development.

### Effects of VEGF Inhibition on Tortuosity and Dilation of Retinal Vessels in the 50/10 OIR model

In the 50/10 OIR model, retinal tortuosity occurs<sup>38</sup> and has similarities to human plus disease, a feature of severe ROP (Figure 10). Historically, the cause of plus disease has been proposed to be increased blood flow from a peripheral mesenchymal shunt in the region where intravitreal neovascularization develops<sup>42</sup>. Chanling et al. found that smooth muscle cell differentiation was altered under relative hypoxia in a kitten model of hyperoxia induced vaso-obliteration and proposed that loss of smooth muscle cells in retinal vessels would contribute to impaired autoregulation of blood flow<sup>65</sup>. Doppler studies of blood flow in the central retinal artery showed either reduced or no difference in blood flow in human infants with or without ROP or with or without plus disease<sup>66,67</sup>. However, these studies are difficult in the awake preterm infant, and measurements at the central retinal artery may not reflect peripheral blood flow, where the mesenchymal shunt is presumed to occur.

Increased blood flow increases shear stress, or the in-line frictional force in a straight vessel. In tortuous vessels, shear stress is believed greater at the acutely curved portion of the vessel. Shear stress can activate endothelial nitric oxide synthetase (eNOS), which then can lead to vessel relaxation and dilation. eNOS can also be activated by hypoxia and VEGF. Ernest had shown that the kitten retina in oxygen-induced retinopathy models was hypoxic during relative hypoxia upon return to room air<sup>7</sup>. We also found that the rat pup retina was hypoxic in the 50/10 OIR model<sup>8</sup> (see below). *eNOS*<sup>-/-</sup> mice subjected to hyperoxia followed by relative hypoxia developed less severe retinopathy, but there was no change in retinal VEGF levels suggesting that VEGF expression was not triggered by eNOS<sup>68</sup>. Therefore, we asked if retinal hypoxia triggered increased expression of VEGF and signaling through VEGFR2 to then trigger eNOS and retinal vessel dilation, a feature of plus disease.

We first determined the time points when arteriolar tortuosity occurred in the 50/10 OIR model by tracing vessels with ROptool version 1.1, from the University of North Carolina Computer-Aided Diagnosis and Display Laboratory<sup>41</sup>. Compared to room air, arteriolar tortuosity was significantly increased at p12 and p14 at the same time points as VEGF was increased (Figure 11). To determine if eNOS was increased in the 50/10 OIR model, we measured western blots for eNOS protein relative to  $\beta$ -actin and phosphorylated eNOS in the 50/10 OIR model compared to room air. eNOS relative to  $\beta$ -actin was significantly

greater at p12 and p14 in 50/10 OIR compared to room air retinas. Therefore, eNOS was expressed to a greater extent at time points when arteriolar tortuosity and VEGF were also increased (p12 and p14).

To determine if eNOS was a downstream regulator of VEGF signaling, we used a neutralizing antibody to VEGF at a dose that we previously found effective in inhibiting intravitreal neovascularization<sup>64</sup>. Compared to a non-immune IgG control, arteriolar tortuosity was significantly reduced by the neutralizing antibody to VEGF (Figure 12). However, neither eNOS nor phosphorylated eNOS was reduced<sup>39</sup>.

We then asked whether VEGF signaling might be leading to dilation in vessels by altering the direction of subsequent endothelial daughter cell migration. Previously, we found that the cleavage planes of endothelial cells during anaphase were disordered when signaling through VEGFR2 was increased using a *flt-1*<sup>-/-</sup> embryonic stem cell model. (*flt-1* is the murine analog of VEGFR1. When knocked out, VEGF cannot bind to VEGFR1 and therefore causes signaling of VEGF to go through VEGFR2.) When a soluble *flt-1* transgene with a PECAM-1 specific promoter was introduced into the model, restoration of the normal orientation of the cleavage planes occurred<sup>69</sup>.

Since we found that inhibition of VEGF signaling through VEGFR2 reduced intravitreal neovascularization<sup>64</sup>, we chose to use a neutralizing antibody as the strategy to reduce VEGF signaling and determine the effect on vessel dilation. To analyze effects on vessel dilation, we measured the angle between the long axis of the vessel and the cleavage plane of dividing lectin stained endothelial cells in retinal flat mounts of pups raised in either room air or the 50/10 OIR model (Figure 13). To determine dividing cells, we stained the cleavage planes during anaphase using phosphohistone. We also measured endothelial cells by staining vessels with lectin. By p11, there were few mitoses recognized in flat mounts of retinas of room air raised pups and most had angles perpendicular to the long axis of the vessel (predicting vessel elongation). However, in the 50/10 OIR model, there were many more mitoses noted and a greater proportion was parallel to the long axis of the vessel (predicting vessel dilation) or disordered (predicting potential disordered angiogenesis). By Chi-square analysis, there were fewer mitosis planes parallel to the long axis of the vessel after treatment with a neutralizing antibody to VEGF than after with an IgG control ( $p < 0.05$ )<sup>39</sup> providing evidence that inhibition of VEGF caused dilated vessels to become more elongated.

Based on these studies, it appeared that VEGF signaling through VEGFR2 contributed to arteriolar tortuosity and venous dilation through the alteration of the angle of the mitotic cleavage planes. eNOS was increased in the 50/10 OIR model but we were unable to find evidence that it was directly downstream of VEGF at the time points determined.

### **Effects of Reactive Oxygen Species on Avascular/total Retinal, VEGF expression, and Intravitreal Neovascularization in the 50/10 OIR Model**

Oxidative stress has been linked to ROP through mechanisms related to oxygenation of retinal tissue in the preterm infant<sup>70-73</sup>. Reactive oxygen species (ROS) can trigger a number of signaling pathways<sup>17,74</sup>. We anticipated that the zone where intravitreal neovascularization occurred would be a region where abutting vascularized and avascular retina would create spatial changes in oxygenated and hypoxic retina. (Fluctuations in oxygen in a model with abutting areas of vascularized and avascular retina may trigger ROS similar to ischemia-reperfusion injury). To study this, we administered to rat pups intraperitoneal injections of pimonadazole (Hypoxyprobe), a soluble protein that forms insoluble conjugates when in an environment of 10 mm Hg oxygen or less. These adducts can be detected with a fluorescently labeled antibody or quantitated by western blot. We

visualized where insoluble pimonidazole existed in retinal flat mounts from postnatal day 4 room air raised pups and postnatal day 18 pups raised in the 50/10 OIR model. (Retinal avascular areas are about 50% in room air at postnatal day 4 and 25% in 50/10 OIR at postnatal day 18 [Table 1]). In the room air animals even within peripheral avascular retina, there was little insoluble pimonidazole (Figure 14a). However, insoluble pimonidazole was present within the peripheral avascular region adjacent to vascularized retina and also in between retinal vessels centrally in the 50/10 OIR model<sup>8</sup> (Figure 14b).

We determined the effects of fluctuations in oxygen on retinal production of end-products of reactive oxygen species (ROS) and found that lipid hydroperoxides tended to increase in the 50/10 OIR model (Figure 15)<sup>17</sup>. At day 18, apocynin, which is believed to reduce ROS through inhibition of the activation of nicotinamide adenine dinucleotide (phosphate) [NADPH] oxidase, significantly reduced the avascular/total retinal area in the 50/10 OIR model compared to control (Figure 15b). Cleaved caspase-3, a downstream effector of both the intrinsic and extrinsic pathways of apoptosis, was also reduced<sup>17</sup> providing evidence that repeated oxygen fluctuations caused apoptosis through NADPH oxidase activation<sup>17</sup>. These data were in line with those of previous studies that reported reduced avascular retina in the 50/10 OIR model following supplementation with manganese superoxide dismutase or vitamins C or E to reduce ROS<sup>75,76</sup>.

Using cell culture to study the effect of hypoxia on signaling pathways of human retinal microvascular endothelial cells (RMVECs), we found that RMVECs exposed to 1% oxygen had activated phospho-Janus Kinase (JNK) compared to room air exposed RMVECs, although apocynin did not significantly inhibit this. JNK signaling is involved in apoptosis and this may be a mechanism for reduced vascular support in the retina which we found in the 50/10 OIR model<sup>8</sup>.

ROS can also trigger signaling of angiogenesis through VEGF or other pathways in several models<sup>8,77,78</sup>. Furthermore, in a meta-analysis of several clinical studies that tested the antioxidant, vitamin E, a 52% overall reduction in the incidence of stage 3 ROP (intravitreal neovascularization) was found in infants with ROP<sup>79</sup>. However, even though repeated oxygen fluctuations tended to increase ROS, neither the antioxidant, n-acetyl cysteine or apocynin, reduced intravitreal neovascularization or VEGF expression in the 50/10 OIR model<sup>17</sup>. Although we and others have found that VEGF signaling pathway is not the only pathway involved in the development of intravitreal neovascularization<sup>80-82</sup>, it is a dominant pathway in conditions in which hypoxia occurs. Retinal hypoxia increased in the 50/10 OIR model<sup>8</sup>. There are no viable knockouts of VEGF or its receptors. We sought a reasonable approach to reduce the effect of VEGF so as to understand the role of other signaling pathways also important to the development of pathological features of avascular retina and intravitreal neovascularization in ROP.

### **Effects of Supplemental Oxygen on VEGF Expression and Intravitreal Neovascularization (50/10+SO OIR model)**

The role of oxygen in ROP is complex. Early in development, high oxygen is toxic to newly developed vessels and leads to vaso-obliteration. In one study, high oxygen disrupted the differentiation of precursors to develop into endothelial cells<sup>83</sup>. However, later in the course of development, high oxygen had less deleterious effects and even beneficial effects in some models<sup>32</sup>. Mice raised in sustained hyperoxia beyond postnatal day (p)12 had less vaso-obliteration and neovascularization compared to mice exposed to the hyperoxia induced vaso-obliteration and angiogenesis model<sup>33</sup>. Also, rats exposed to oxygen fluctuations and recovered in supplemental oxygen (28%) rather than room air had reduced intravitreal neovascularization at some but not later time points<sup>1</sup>. However, the Supplemental Therapeutic Oxygen for Prethreshold ROP (STOP-ROP) multicenter clinical trial did not



find an overall significant benefit from supplemental oxygen given to human infants with prethreshold ROP<sup>34</sup>. In addition, current clinical studies show that both fluctuations in oxygen as well as increased inspired oxygen of infants, later in their courses in neonatal intensive care units, are associated with higher risk of severe ROP<sup>22–25,27</sup>. Since reducing oxygen is of concern to brain development in preterm infants, and increasing the inspired oxygen is a common practice during preterm infant examinations and procedures in the neonatal intensive care units, knowledge of the effects of supplemental oxygen (SO) on ROP is important.

We studied the effects of recovery in 28% oxygen following repeated oxygen fluctuations (50/10 OIR+SO model) compared to 21% oxygen (50/10 OIR model) on NADPH oxidase activation and the features of avascular retina and intravitreal neovascularization. We found that supplemental oxygen significantly reduced VEGF retinal concentration to levels similar to room air raised animals (Figure 16)<sup>8</sup>. Therefore, using supplemental oxygen in the model following oxygen fluctuations was a way to reduce the effect of VEGF and study alternate pathways.

Although VEGF expression was reduced, supplemental oxygen did not reduce the concentration of conjugated retinal pimonidazole, a marker of retinal hypoxia<sup>8</sup>. The presence of retinal hypoxia while VEGF expression was reduced in the 50/10 OIR model after recovery in supplemental oxygen was unexpected. Our hypothesis is that there is a mismatch of metabolic demand, which increases as photoreceptors develop, and insufficient vascular support. Previously, supplemental oxygen was shown to reduce the autoregulatory effect of retinal vessels in the 50/10 OIR model<sup>1</sup>. In high oxygen this may result in poor constriction of retinal vessels and thus high blood flow and retinal arteriolar oxygen concentration, similar to that suggested in reports in a kitten model of hyperoxia induced vaso-obliteration and angiogenesis<sup>7</sup>. We suspect that increased oxygen within the retina may reduce the stimulus for neurosensory retinal VEGF overexpression, shown by in situ hybridization to occur in Mueller cells and ganglion cells<sup>84</sup>. However, as photoreceptor development occurs, metabolic demand increases and oxygen is required<sup>85,86</sup>. Although oxygen would be increased in the retinal circulation, the choroid, which supplies much oxygen to the eye, is unable to increase oxygen tension in response to supplemental inspired oxygen in the p15 rat (unlike in the adult)<sup>87</sup>. Therefore, although metabolism may increase under greater retinal vascular oxygen, demand may not be met by the choroid. We continue to pursue this area of study.

In the 50/10 OIR+SO model compared to the 50/10 OIR model, supplemental oxygen exacerbated NAD(P)H oxidase activation thus contributing to the area of intravitreal neovascularization<sup>8</sup> (Figure 17). We did not find that Akt or ERK were activated in RMVECs exposed to hypoxia<sup>8</sup>. We therefore determined whether NADPH oxidase activation was working through other angiogenic pathways. The Janus kinase-signal transducer and activator of transcription (JAK/STAT) signaling pathway can lead to angiogenesis through ROS either through VEGF<sup>88,89</sup> or alternate pathways<sup>90,91</sup>. We used a chemical compound that potently inhibits JAK2 protein tyrosine kinase. AG490 (LC Laboratories, Woburn, MA), blocks the constitutive activation of STAT3<sup>92</sup> and selectively inhibits the JAK/STAT pathway in rats<sup>93</sup>. We found that phosphorylated JAK2 and STAT3 were inhibited at p7 and p14 after repeated oxygen fluctuations and at p18 after exposure to supplemental oxygen in the rat pups. Furthermore, after exposure to supplemental oxygen at p18, AG490 significantly reduced the area of intravitreal neovascularization compared to control (Figure 18). Although we found that apocynin significantly reduced phosphorylated STAT3 in the 50/10+SO OIR model (as well as the area of intravitreal neovascularization), there was no difference in the phosphorylation of JAK2 by apocynin. Furthermore, neither apocynin nor AG490 significantly affected retinal VEGF in the 50/10 OIR+SO model.

However the concentration of VEGF in the retinas in the 50/10 OIR +SO model was 10 fold lower than in the 50/10 OIR model and at the concentration in retinas of room air raised rats of the same postnatal day ages<sup>94</sup>. Thus, supplemental oxygen, which clinically may be related to more severe human ROP, also permitted us to begin to understand the effect of other signaling pathways that may contribute to intravitreal neovascularization when VEGF levels are not elevated.

## Summary

We have found that the oxygen extremes and the appearance of the retina in the 50/10 OIR model mimics ROP seen today and differs from earlier models of oxygen-induced retinopathy developed to study ROP when it was initially described in the 1940's. Whereas hyperoxia induced avascular retina is associated with reduced VEGF in the mouse model<sup>52</sup>, avascular retina in the 50/10 OIR model has increased VEGF concentrations compared to room air at the same time points. Increased signaling through VEGFR2 causes intravitreal neovascularization, but it is not the sole cause of it. Inhibition of VEGF bioactivity by a neutralizing antibody to VEGF reduces VEGFR2 signaling and inhibits intravitreal neovascularization, retinal tortuosity and dilation, without interfering with ongoing intraretinal neovascularization. But concerns remain because VEGF is a survival factor for neurons and endothelial cells so use in preterm infants requires careful study.

We found that ROS were increased by repeated oxygen fluctuations and led to increased avascular retina through NADPH oxidase induced apoptosis. Recovery from oxygen fluctuations in supplemental oxygen exacerbated NADPH oxidase to contribute to intravitreal neovascularization, during reduced retinal VEGF, through pathways involving the JAK/STAT pathway. Therefore, in the complex oxygen environment of the preterm infant several angiogenic and apoptotic pathways appear involved to lead to avascular retina through apoptosis and intravitreal neovascularization.

By understanding pathways of avascular retina and intravitreal neovascularization that involve VEGF or are triggered even when VEGF is not overexpressed, we expand our treatment possibilities to include safer ones and avoid concerns of inhibiting the survival aspects of VEGF in the developing infant. Also, the oxygen stresses (oxygen fluctuations, hypoxia, hyperoxia and supplemental oxygen) are relevant to today's preterm infant. Greater study of pathways involved during different oxygen stresses may also be important to determine effective selective treatments.

## Acknowledgments

Grant Funding: (MEH, PI): NIH/NEI EY015130, EY017011; March of Dimes; American Diabetes Association; Research to Prevent Blindness

## Reference List

1. Berkowitz BA, Zhang W. Significant reduction of the panretinal oxygenation response after 28% supplemental oxygen recovery in experimental ROP. *Invest Ophthalmol Vis Sci.* 2000; 41:1925–1931. [PubMed: 10845618]
2. McColm, JR.; Hartnett, ME. *Pediatric Retinal Diseases: Medical and Surgical Approaches.* Philadelphia: Lippincot Williams & Wilkins; 2005. Retinopathy of prematurity: current understanding based on clinical trials and animal models; p. 387-409.
3. Cryotherapy for Retinopathy of Prematurity Cooperative Group. Multicenter Trial of Cryotherapy for Retinopathy of Prematurity Ophthalmological Outcomes at 10 Years. *Arch Ophthalmol.* 2001; 119:1110–1118. [PubMed: 11483076]

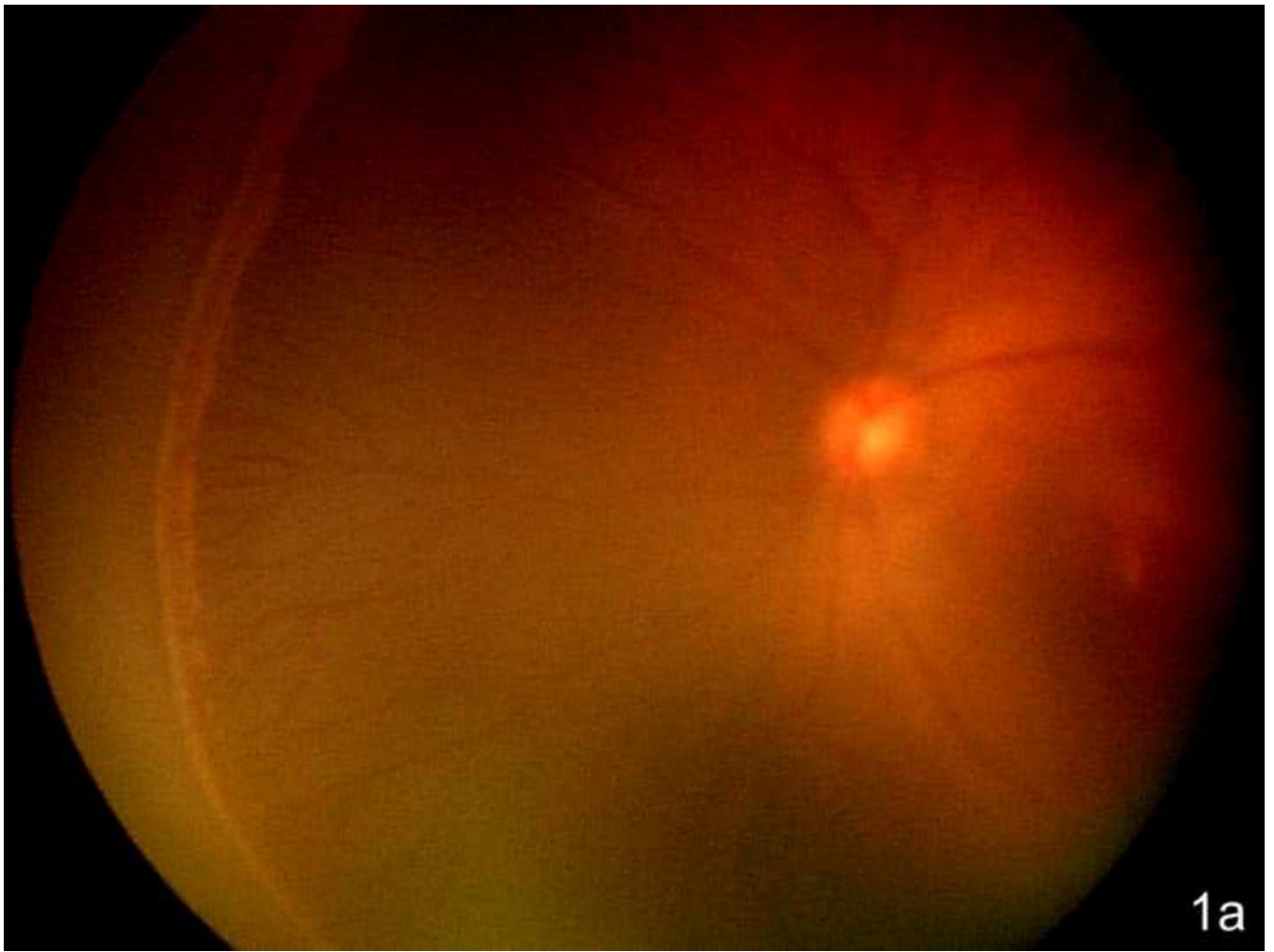
4. Early Treatment for Retinopathy of Prematurity Cooperative Group. Revised indications for the treatment of retinopathy of prematurity: results of the early treatment for retinopathy of prematurity randomized trial. *Arch Ophthalmol*. 2003; 121:1684–1694. [PubMed: 14662586]
5. Flynn JT. Retinopathy of prematurity. *Ped Clin N Am*. 1987; 34:1487–1516.
6. Cryotherapy for Retinopathy of Prematurity Cooperative Group. Multicenter trial of cryotherapy for retinopathy of prematurity: natural history ROP: ocular outcome at 5(1/2) years in premature infants with birth weights less than 1251g. *Arch Ophthalmol*. 2002; 120:595–599. [PubMed: 12003608]
7. Ernest JT, Goldstick TK. Retinal oxygen tension and oxygen reactivity in retinopathy of prematurity in kittens. *Invest Ophthalmol Vis Sci*. 1984; 25:1129–1134. [PubMed: 6207136]
8. Saito Y, Uppal A, Byfield G, Budd S, Hartnett ME. Activated NAD(P)H Oxidase from Supplemental Oxygen Induces Neovascularization Independent of VEGF in Retinopathy of Prematurity Model. *Investigative Ophthalmology Visual Science*. 2008; 49:1591–1598. [PubMed: 18385079]
9. Terry TL. Extreme prematurity and fibroblastic overgrowth of persistent vascular sheath behind each crystalline lens:(1) Preliminary report. *Am J Ophthalmol*. 1942; 25:203–204.
10. Wang S, Sorenson CM, Sheibani N. Attenuation of retinal vascular development and neovascularization during oxygen-induced ischemic retinopathy in Bcl-2<sup>-/-</sup> mice. *Developmental Biology*. 2005; 279:205–219. [PubMed: 15708569]
11. Shih SC, Ju M, Liu N, Smith LEH. Selective stimulation of VEGFR-1 prevents oxygen-induced retinal vascular degeneration in retinopathy of prematurity. *J Clin Invest*. 2003; 112:50. [PubMed: 12840058]
12. Alon T, et al. Vascular endothelial growth factor acts as a survival factor for newly formed retinal vessels and has implications for retinopathy of prematurity. *Nat Med*. 1995; 1:1024–1028. [PubMed: 7489357]
13. Chang KH, et al. IGF binding protein-3 regulates hematopoietic stem cell and endothelial precursor cell function during vascular development. *PNAS*. 2007; 104:10595–10600. [PubMed: 17567755]
14. Lofqvist C, et al. From the Cover: IGFBP3 suppresses retinopathy through suppression of oxygen-induced vessel loss and promotion of vascular regrowth. *PNAS*. 2007; 104:10589–10594. [PubMed: 17567756]
15. Connor KM, et al. Increased dietary intake of [omega]-3-polyunsaturated fatty acids reduces pathological retinal angiogenesis. *Nat Med*. 2007; 13:868–873. [PubMed: 17589522]
16. Neu J, et al. The Dipeptide Arg-Gln Inhibits Retinal Neovascularization in the Mouse Model of Oxygen-Induced Retinopathy. *Investigative Ophthalmology Visual Science*. 2006; 47:3151–3155. [PubMed: 16799062]
17. Saito Y, Geisen P, Uppal A, Hartnett ME. Inhibition of NAD(P)H oxidase reduces apoptosis and avascular retina in an animal model of retinopathy of prematurity. *Mol Vis*. 2007; 13:840–853. [PubMed: 17615545]
18. Ashton N, Cook C. Direct observation of the effect of oxygen on developing vessels: preliminary report. *Br J Ophthalmol*. 1954; 38:433–440. [PubMed: 13172418]
19. Patz A, Eastham A, Higginbotham DH, Kleh T. Oxygen studies in retrolental fibroplasia. *Am J Ophthalmol*. 1953; 36:1511–1522. [PubMed: 13104558]
20. Michaelson IC. The mode of development of the vascular system of the retina. With some observations on its significance for certain retinal diseases. *Trans Ophthal Soc UK*. 1948; 68:137–180.
21. Patz A. The effect of oxygen on immature retinal vessels. [Review] [23 refs]. *Investigative Ophthalmology*. 1965; 4:988–999. [PubMed: 5321926]
22. Cunningham S, Fleck BW, Elton RA, McIntosh N. Transcutaneous oxygen levels in retinopathy of prematurity. *Lancet*. 1995; 346:1464–1465. [PubMed: 7490994]
23. McColm JR, et al. Hypoxic oxygen fluctuations produce less severe retinopathy than hyperoxic fluctuations in a rat model of retinopathy of prematurity. *Pediatr Res*. 2004; 55:107–113. [PubMed: 14561784]
24. Saito Y, et al. The progression of retinopathy of prematurity and fluctuation in blood gas tension. *Graefes Arch Clin Exper Ophthalmol*. 1993; 231:151–156. [PubMed: 8462887]

25. Chow LC, Wright KW, Sola A. Can changes in clinical practice decrease the incidence of severe retinopathy of prematurity in very low birth weight infants? *Pediatrics*. 2003; 111:339–345. [PubMed: 12563061]
26. Wedrychowicz A, Dziatkowiak H, Nazim J, Sztefko K. Insulin-like growth factor-1 and its binding proteins, IGFBP-1 and IGFBP-3, in adolescents with type-1 diabetes mellitus and microalbuminuria. *Horm Res*. 2005; 63(5):245–299. [PubMed: 15920342]
27. Tin W, Milligan DWA, Pennefather PM, Hey E. Pulse oximetry, severe retinopathy, and outcome at one year in babies of less than 28 weeks gestation. *Arch Dis Child Fetal Neonat Ed*. 2001; 84:106–110.
28. Werdich XQ, McCollum GW, Rajaratnam VS, Penn JS. Variable oxygen and retinal VEGF levels: correlation with incidence and severity of pathology in a rat model of oxygen-induced retinopathy. *Exp Eye Res*. 2004; 79:623–630. [PubMed: 15500821]
29. McColm JR, Cunningham S, Yerden R. A computer controlled system to simulate the small, rapid oxygen fluctuations experienced by preterm infants developing retinopathy of prematurity. *Scottish Medical Journal*. 1999; 44(1):28–29. abstract.
30. Pierce EA, Avery RL, Foley ED, Aiello LP, Smith LEH. Vascular endothelial growth factor/vascular permeability factor expression in a mouse model of retinal neovascularization. *Proc Natl Acad Sci USA*. 1995; 92:905–909. [PubMed: 7846076]
31. Penn JS, Henry MM, Wall PT, Tolman BL. The range of PaO<sub>2</sub> variation determines the severity of oxygen induced retinopathy in newborn rats. *Invest Ophthalmol Vis Sci*. 1995; 36:2063–2070. [PubMed: 7657545]
32. Phelps DL. Reduced severity of oxygen-induced retinopathy in kittens recovered in 28% oxygen. *Pediatr Res*. 1988; 24:106–109. [PubMed: 3412844]
33. Gu X, et al. Effects of sustained hyperoxia on revascularization in experimental retinopathy of prematurity. *Invest Ophthalmol Vis Sci*. 2002; 43:496–502. [PubMed: 11818396]
34. STOP-ROP Multicenter Study Group. Supplemental Therapeutic Oxygen for Prethreshold Retinopathy of Prematurity (STOP-ROP), a randomized, controlled trial. I: primary outcomes. *Pediatrics*. 2000; 105:295–310. [PubMed: 10654946]
35. Wallace DK, Veness-Meehan KA, Miller WC. Incidence of severe retinopathy of prematurity before and after a modest reduction in target oxygen saturation levels. *Journal of American Association for Pediatric Ophthalmology and Strabismus*. 2007; 11:170–174. [PubMed: 17416327]
36. Vanderveen DK, Mansfield TA, Eichenwald EC. Lower Oxygen Saturation Alarm Limits Decrease the Severity of Retinopathy of Prematurity. *Journal of American Association for Pediatric Ophthalmology and Strabismus*. 2006; 10:445–448. [PubMed: 17070480]
37. Penn JS, Henry MM, Tolman BL. Exposure to alternating hypoxia and hyperoxia causes severe proliferative retinopathy in the newborn rat. *Pediatr Res*. 1994; 36:724–731. [PubMed: 7898981]
38. Liu K, Akula JD, Falk C, Hansen RM, Fulton AB. The Retinal Vasculature and Function of the Neural Retina in a Rat Model of Retinopathy of Prematurity. *Investigative Ophthalmology Visual Science*. 2006; 47:2639–2647. [PubMed: 16723481]
39. Hartnett ME, et al. Neutralizing VEGF decreases tortuosity and alters endothelial cell division orientation in arterioles and veins in rat model of ROP: Relevance to plus disease. *Invest Ophthalmol Vis Sci*. Mar 31.2008 epub.
40. Werdich XQ, Penn JS. Specific Involvement of Src Family Kinase Activation in the Pathogenesis of Retinal Neovascularization. *Investigative Ophthalmology Visual Science*. 2006; 47:5047–5056. [PubMed: 17065526]
41. Aylward SR, Bullitt E. Initialization, noise, singularities, and scale in height ridge traversal for tubular object centerline extraction. *IEEE Trans.Med.Imaging*. 2002; 21:61–75. [PubMed: 11929106]
42. Chan-Ling T, Gock B, Stone J. The effect of oxygen on vasoformative cell division: Evidence that 'physiological hypoxia' is the stimulus for normal retinal vasculogenesis. *Invest Ophthalmol Vis Sci*. 1995; 36:1201–1214. [PubMed: 7775098]

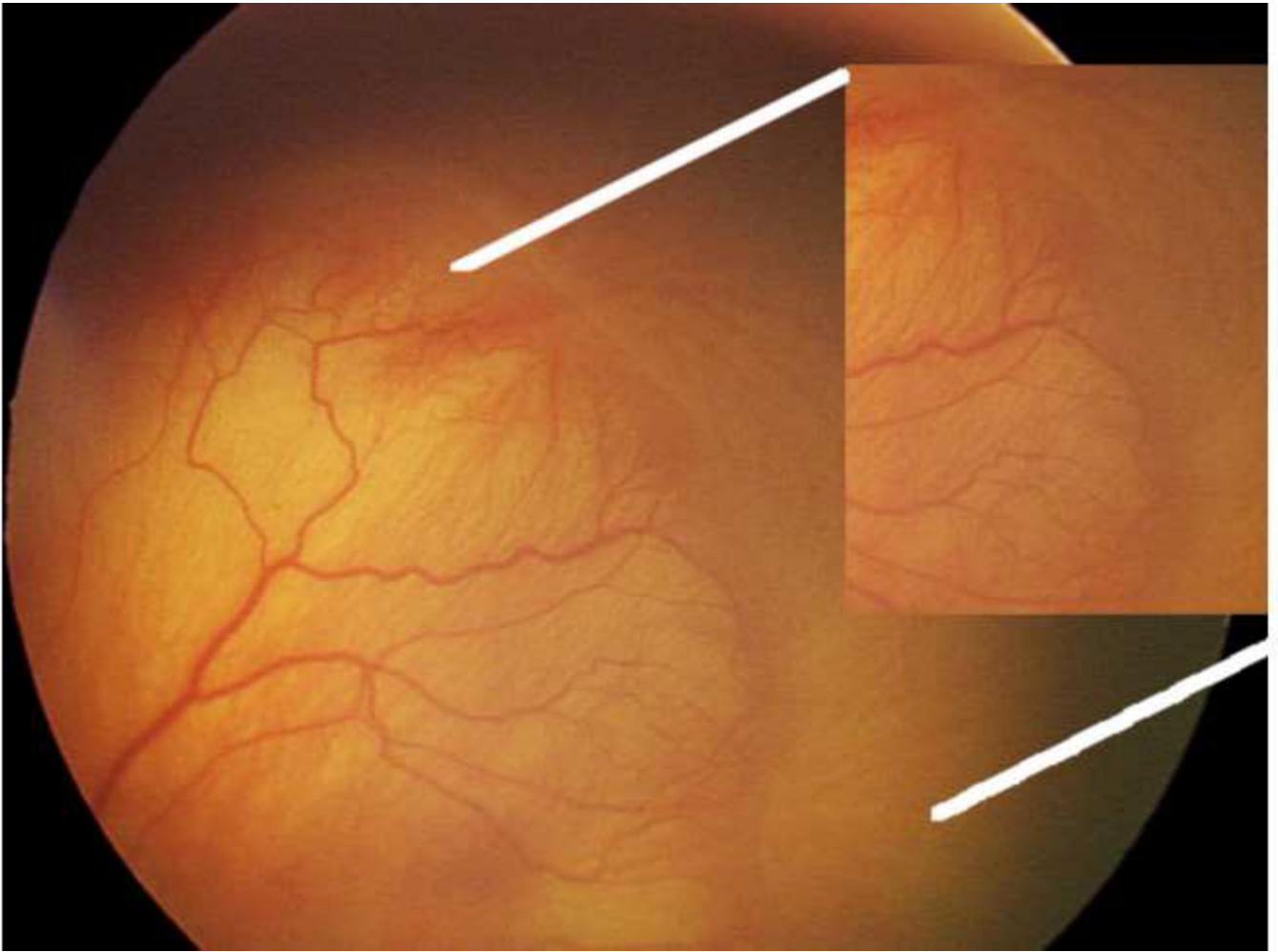
43. Stone J, et al. Development of retinal vasculature is mediated by hypoxia-induced vascular endothelial growth factor (VEGF) expression by neuroglia. *J Neurosci.* 1995; 15:4738–4747. [PubMed: 7623107]
44. Saint-Geniez M, Maldonado AE, D'Amore PA. VEGF Expression and Receptor Activation in the Choroid during Development and in the Adult. *Investigative Ophthalmology Visual Science.* 2006; 47:3135–3142. [PubMed: 16799060]
45. Maharaj ASR, Saint-Geniez M, Maldonado AE, D'Amore PA. Vascular Endothelial Growth Factor Localization in the Adult. *Am J Path.* 2006; 168:639–648. [PubMed: 16436677]
46. Robinson GS, Aiello LP. Angiogenic factors in diabetic ocular disease: Mechanisms of today, therapies for tomorrow. *International Ophthalmology Clinics.* 1998; 38:89–102. [PubMed: 9604739]
47. Adamis AP, et al. Increased vascular endothelial growth factor levels in the vitreous of eyes with proliferative diabetic retinopathy. *Am J Ophthalmol.* 1994; 118:445–450. [PubMed: 7943121]
48. Dawson DW, et al. Pigment epithelium-derived factor: a potent inhibitor of angiogenesis. *Science.* 1999; 285:245–248. [PubMed: 10398599]
49. Duh EJ, et al. Pigment epithelium-derived factor suppresses ischemia-induced retinal neovascularization and VEGF-induced migration and growth. *Invest Ophthalmol Vis Sci.* 2002; 43:821–829. [PubMed: 11867604]
50. Mori K, et al. Regression of ocular neovascularization in response to increased expression of pigment epithelium-derived factor. *Invest Ophthalmol Vis Sci.* 2002; 43:2428–2434. [PubMed: 12091447]
51. Gao G, et al. Down-regulation of vascular endothelial growth factor and up-regulation of pigment epithelium-derived factor. A possible mechanism for the anti-angiogenesis activity of plasminogen kringle 5. *J Biol Chem.* 2002; 277:9492. [PubMed: 11782462]
52. Pierce E, Foley E, Lois EH. Regulation of vascular endothelial growth factor by oxygen in a model of retinopathy of prematurity. *Arch Ophthalmol.* 1996; 114:1219–1228. [PubMed: 8859081]
53. Ishida S, et al. VEGF164-mediated inflammation is required for pathological, but not physiological, ischemia-induced retinal neovascularization. *J Exp Med.* 2003; 198:483–489. [PubMed: 12900522]
54. Usui T, et al. VEGF164(165) as the pathological isoform: differential leukocyte and endothelial responses through VEGFR1 and VEGFR2. *Invest Ophthalmol Vis Sci.* 2004; 45:368–374. [PubMed: 14744874]
55. Lee S, Jilani SM, Nikolova GV, Carpizo D, Iruela-Arispe ML. Processing of VEGF-A by matrix metalloproteinases regulates bioavailability and vascular patterning in tumors. *J. Cell Biol.* 2005; 169:681–691. [PubMed: 15911882]
56. Stalmans I, et al. Arteriolar and venular patterning in retinas of mice selectively expressing VEGF isoforms. *J Clin Invest.* 2002; 109:327–336. [PubMed: 11827992]
57. Carmeliet P, et al. Impaired myocardial angiogenesis and ischemic cardiomyopathy in mice lacking the vascular endothelial growth factor isoforms VEGF164 and VEGF188. *Nat Med.* 1999; 5:495–501. [PubMed: 10229225]
58. Ng YS, Rohan R, Sunday ME, Demello DE, D'Amore PA. Differential expression of VEGF isoforms in mouse during development and in the adult. *Dev Dyn.* 2001; 220:112–121. [PubMed: 11169844]
59. Tischer E, et al. The human gene for vascular endothelial growth factor. Multiple protein forms are encoded through alternative exon splicing. *J Biol Chem.* 1991; 266:11947–11954. [PubMed: 1711045]
60. Ruhrberg C, et al. Spatially restricted patterning cues provided by heparin-binding VEGF-A control blood vessel branching morphogenesis. *Genes & Development.* 2002; 16:2684–2698. [PubMed: 12381667]
61. Hutchings H, Ortega N, Plouet J. Extracellular matrix-bound vascular endothelial growth factor promotes endothelial cell adhesion, migration, and survival through integrin ligation. *FASEB J.* 2003 02-0691fje.

62. McColm JR, Geisen P, Hartnett ME. VEGF isoforms and their expression after a single episode of hypoxia or repeated fluctuations between hyperoxia and hypoxia: Relevance to clinical ROP. *Mol Vis*. 2004; 10:512–520. [PubMed: 15303088]
63. Gerhardt H, et al. VEGF guides angiogenic sprouting utilizing endothelial tip cell filopodia. *J Cell Biol*. 2003; 161:1163–1177. [PubMed: 12810700]
64. Geisen P, et al. Neutralizing antibody to VEGF reduces intravitreal neovascularization and does not interfere with vascularization of avascular retina in an ROP model. *Molecular Vision*. 2008; 14:345–357. Ref Type: Journal (Full). [PubMed: 18334951]
65. Hughes S, Gardiner T, Baxter L, Chan-Ling T. Changes in Pericytes and Smooth Muscle Cells in the Kitten Model of Retinopathy of Prematurity: Implications for Plus Disease. *Investigative Ophthalmology Visual Science*. 2007; 48:1368–1379. [PubMed: 17325186]
66. Holland D, et al. Color Doppler imaging of the central retinal artery in premature infants undergoing examination for retinopathy of prematurity. *Journal of AAPOS*. 1999; 3:194–198. [PubMed: 10477220]
67. Niwald A, Gralek M. Evaluation of blood flow in the ophthalmic artery and central retinal artery in children with retinopathy of prematurity. *Klinika oczna*. 2006; 108:32–35. [PubMed: 16883936]
68. Brooks SE, et al. Reduced severity of oxygen-induced retinopathy in eNOS-deficient mice. *Invest Ophthalmol Vis Sci*. 2001; 42:222–228. [PubMed: 11133872]
69. Zeng G, et al. Orientation of endothelial cell division is regulated by VEGF signaling during blood vessel formation. *Blood*. 2007; 109:1345–1352. [PubMed: 17068148]
70. Katz ML, Robison WG Jr. Autoxidative damage to the retina: Potential role in retinopathy of prematurity. *Birth Defects*. 1988; 24:237–248. [PubMed: 2846086]
71. Penn JS. Oxygen-induced retinopathy in the rat: possible contribution of peroxidation reactions. *Doc Ophthalmol*. 1990; 74:179–186. [PubMed: 2209375]
72. Phelps DL, Rosenbaum AL. Observations of vitamin E in experimental oxygen-induced retinopathy. *Ophthalmology*. 1979; 86:1741–1748. [PubMed: 95420]
73. Penn JS, Tolman BL, Lowery LA. Variable oxygen exposure causes preretinal neovascularisation in the newborn rat. *Invest Ophthalmol Vis Sci*. 1993; 34:576–585. [PubMed: 8449677]
74. Ushio-Fukai M. Redox signaling in angiogenesis: Role of NADPH oxidase. *Cardiovasc Res*. 2006; 71:226–235. [PubMed: 16781692]
75. Niesman MR, Johnson KA, Penn JS. Therapeutic effect of liposomal superoxide dismutase in an animal model of retinopathy of prematurity. *Neurochemical Research*. 1997; 22:597–605. [PubMed: 9131639]
76. Penn JS. Oxygen-induced retinopathy in the rat Vitamins C and E as potential therapies. *Invest Ophthalmol Vis Sci*. 1992; 33:1836–1845. [PubMed: 1582786]
77. Jay Forman H, Torres M. Redox signaling in macrophages. *Molecular Aspects of Medicine*. 2001; 22:189–216. [PubMed: 11679166]
78. Al Shabrawey M, et al. Inhibition of NAD(P)H Oxidase activity blocks vascular endothelial growth factor overexpression and neovascularization during ischemic retinopathy. *Am J Path*. 2005; 167:599–607. [PubMed: 16049343]
79. Raju TNK, Langenberg P, Bhutani V, Quinn GE. Vitamin E prophylaxis to reduce retinopathy of prematurity: A reappraisal of published trials. *J Pediatr*. 1997; 131:844–850. [PubMed: 9427888]
80. Kramerov AA, et al. Expression of Protein Kinase CK2 in Astroglial Cells of Normal and Neovascularized Retina. *Am J Path*. 2006; 168:1722–1736. [PubMed: 16651637]
81. Dorrell MI, Aguilar E, Schepke L, Barnett FH, Friedlander M. Combination angiostatic therapy completely inhibits ocular and tumor angiogenesis. *PNAS*. 2007; 104:967–972. [PubMed: 17210921]
82. Jo N, et al. Inhibition of Platelet-Derived Growth Factor B Signaling Enhances the Efficacy of Anti-Vascular Endothelial Growth Factor Therapy in Multiple Models of Ocular Neovascularization. *Am J Path*. 2006; 168:2036–2053. [PubMed: 16723717]
83. Uno K, Merges CA, Grebe R, Luty GA, Prow TW. Hyperoxia inhibits several critical aspects of vascular development. *Dev Dyn*. 2007; 236:981–990. [PubMed: 17366630]

84. Robinson GS, et al. Oligodeoxynucleotides inhibit retinal neovascularization in a murine model of proliferative retinopathy. *Proc Natl Acad Sci USA*. 1996; 93:4851–4856. [PubMed: 8643492]
85. Akula JD, Hansen RM, Martinez-Perez ME, Fulton AB. Rod Photoreceptor Function Predicts Blood Vessel Abnormality in Retinopathy of Prematurity. *Investigative Ophthalmology Visual Science*. 2007; 48:4351–4359. [PubMed: 17724227]
86. Berkowitz BA, Roberts R, Penn JS, Gradianu M. High-Resolution Manganese-Enhanced MRI of Experimental Retinopathy of Prematurity. *Investigative Ophthalmology Visual Science*. 2007; 48:4733–4740. [PubMed: 17898298]
87. Cringle SJ, Yu PK, Su EN, Yu DY. Oxygen Distribution and Consumption in the Developing Rat Retina. *Investigative Ophthalmology Visual Science*. 2006; 47:4072–4076. [PubMed: 16936126]
88. Ushio-Fukai M, Alexander RW. Reactive oxygen species as mediators of angiogenesis signaling. Role of NAD(P)H oxidase. *Molecular and Cellular Biochemistry*. 2004; 264:85–97. [PubMed: 15544038]
89. Ushio-Fukai M. VEGF Signaling Through NADPH Oxidase-Derived ROS. *Antioxidants & Redox Signaling*. 2007; 9:731–739. [PubMed: 17511588]
90. Liu T, et al. Reactive Oxygen Species Mediate Virus-induced STAT Activation: ROLE OF TYROSINE PHOSPHATASES. *J Biol Chem*. 2004; 279:2461–2469. [PubMed: 14578356]
91. Lee YJ, Heo JS, Suh HN, Lee MY, Han HJ. Interleukin-6 stimulates  $\alpha$ -MG uptake in renal proximal tubule cells: involvement of STAT3, PI3K/Akt, MAPKs, and NF- $\kappa$ B. *Am J Physiol Renal Physiol*. 2007; 293:F1036–F1046. [PubMed: 17581928]
92. Levitzki A. Tyrosine phosphatases—potential antiproliferative agents and novel molecular tools. *Biochem Pharmacol*. 2008; 40:913–918. [PubMed: 2143901]
93. Banas AK, et al. Angiotensin II blockade prevents hyperglycemia-induced activation of JAK and STAT proteins in diabetic rat kidney glomeruli. *Am J Physiol Renal Physiol*. 2004; 286:F653–F659. [PubMed: 14678947]
94. Byfield G, Budd S, Hartnett ME. Supplemental oxygen can cause intravitreal neovascularization through JAK/STAT pathways in a model of retinopathy of prematurity. *Investigative Ophthalmology & Visual Science*. 2009 in press.

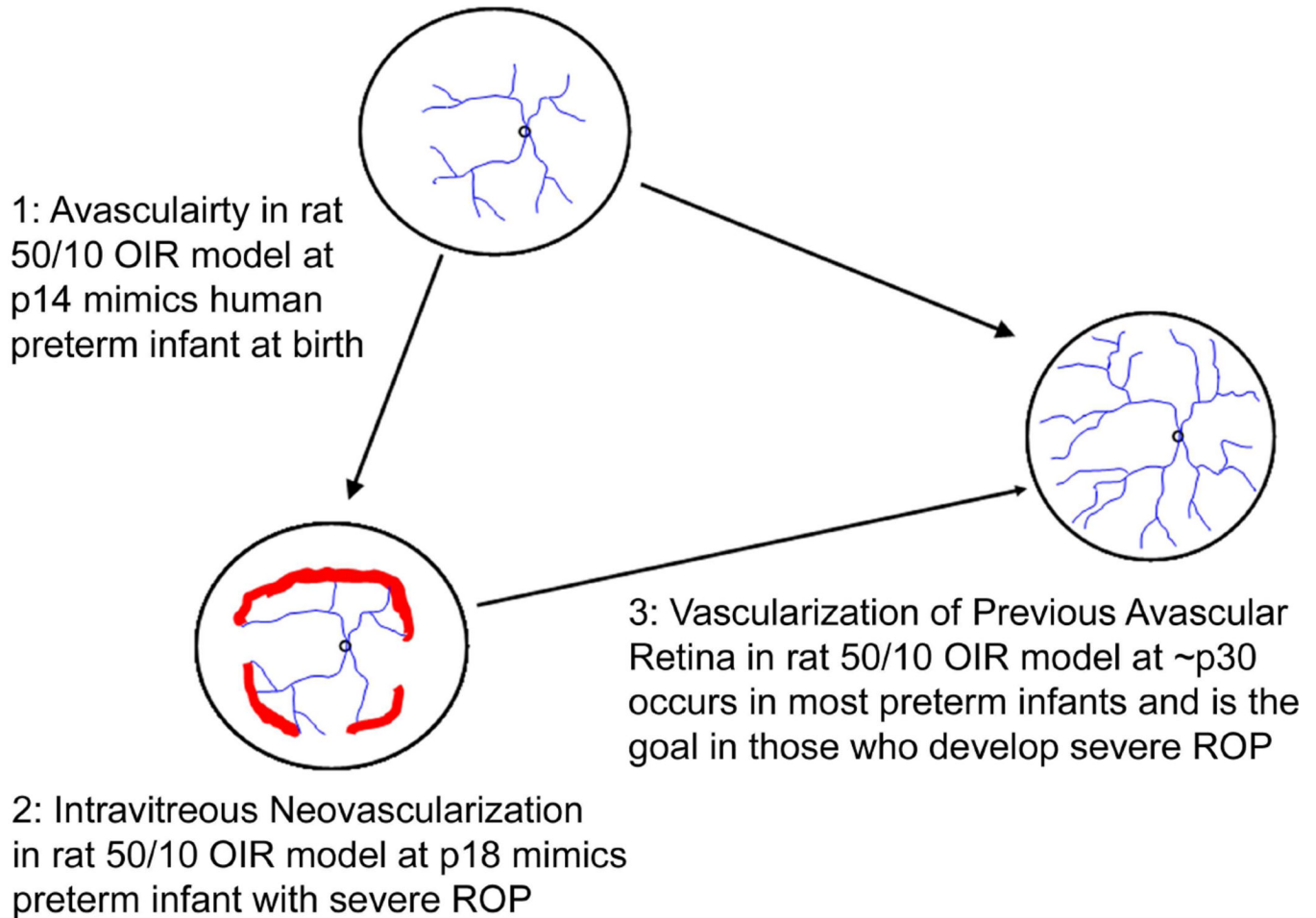






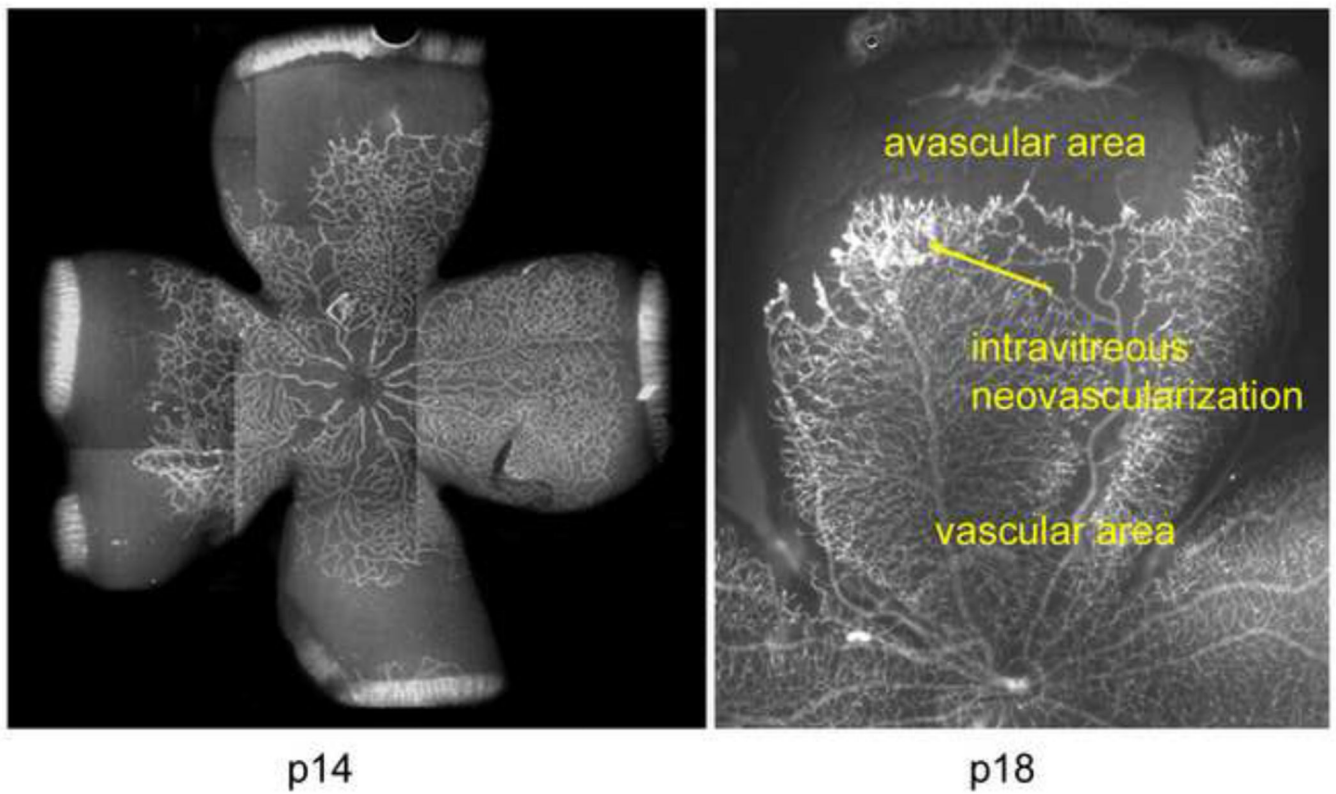
**Figure 1.**

- a. Zone II with ridge in the nasal periphery of the left eye of a preterm infant showing early stage 3 ROP, or intravitreal neovascularization (Retacam image, Clarity, CA).
- b. Left eye of preterm infant with stage 3 ROP (intravitreal neovascularization) showing flat neovascularization that can occur in zone I and posterior zone II ROP. (see inset zoomed image; Retacam image, Clarity, CA).



**Figure 2.**

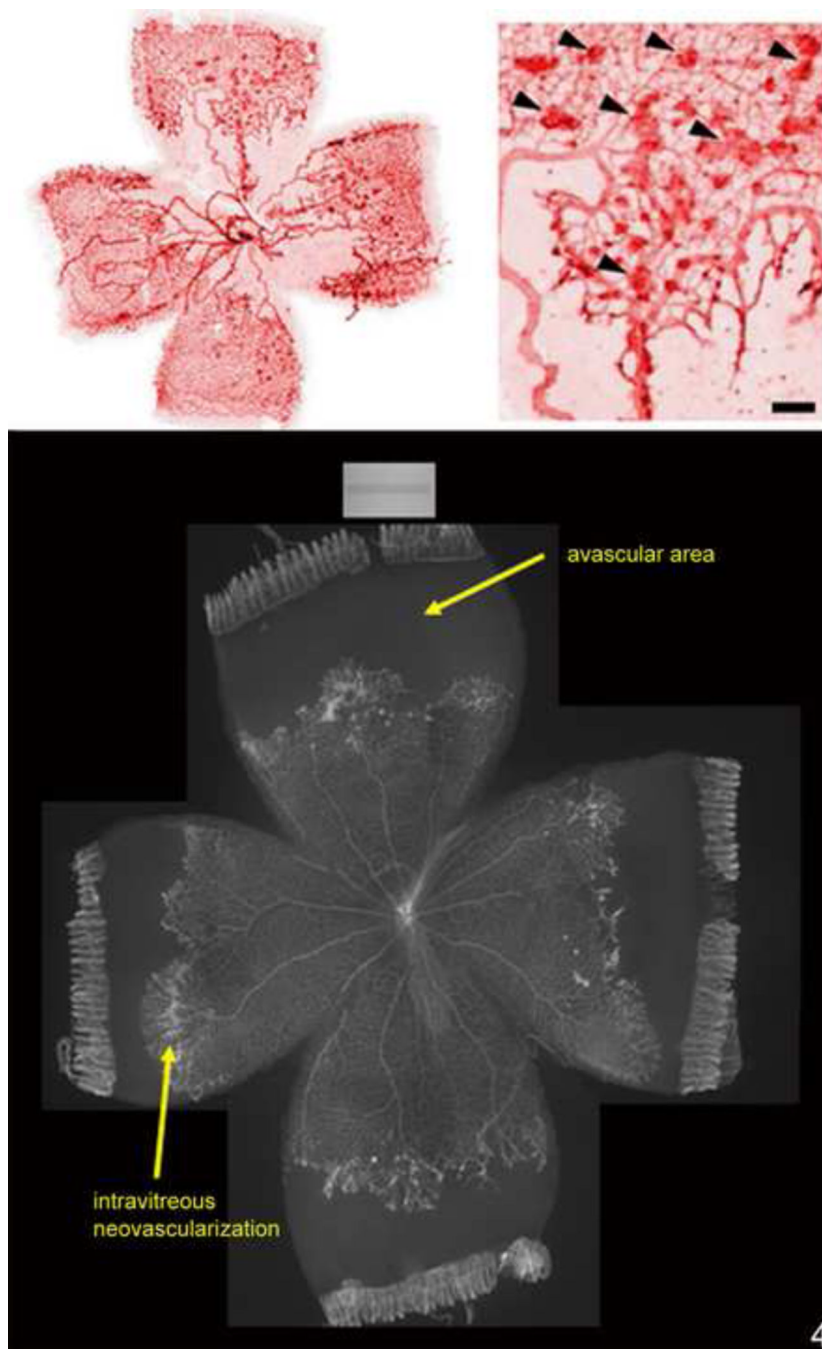
50/10 OIR model at different post-natal day ages (p) mimics what occurs in human preterm infants. (1) at birth, human preterm infants have incompletely vascularized retina; (2) approximately 6% of preterm infants born less than 1000 grams in birth weight will develop severe ROP, at which time treatment with laser is recommended to reduce unwanted intravitreal neovascularization and consequences of retinal detachment; (3) most preterm infants will undergo vascularization of the avascular retina and 50% of infants with threshold severe ROP will also have regression of the intravitreal neovascularization with ongoing vascularization of the avascular retina. The goal of our lab is to promote vascularization of avascular retina and to reduce unwanted intravitreal neovascularization.



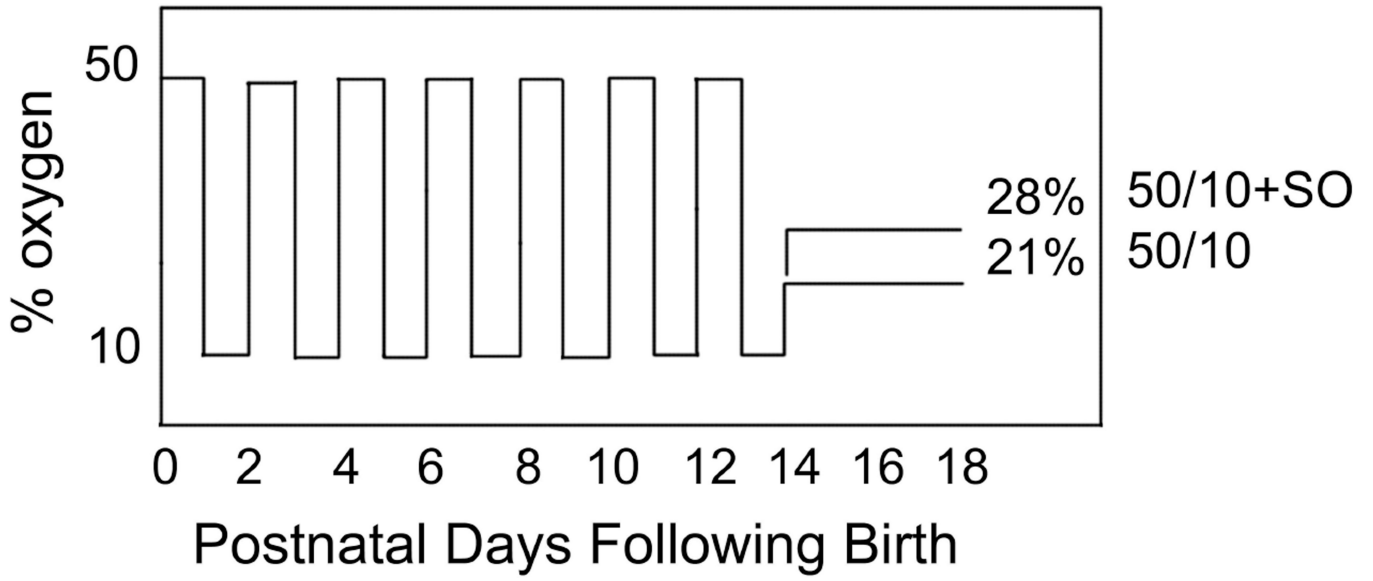
**Figure 3.**

A. Lectin-stained retinal flat mount of pup in 50/10 OIR model at postnatal day (p)14 after 7 cycles of oxygen fluctuations between 50% and 10% inspired oxygen showing peripheral avascular retina, similar to that in zone II ROP.

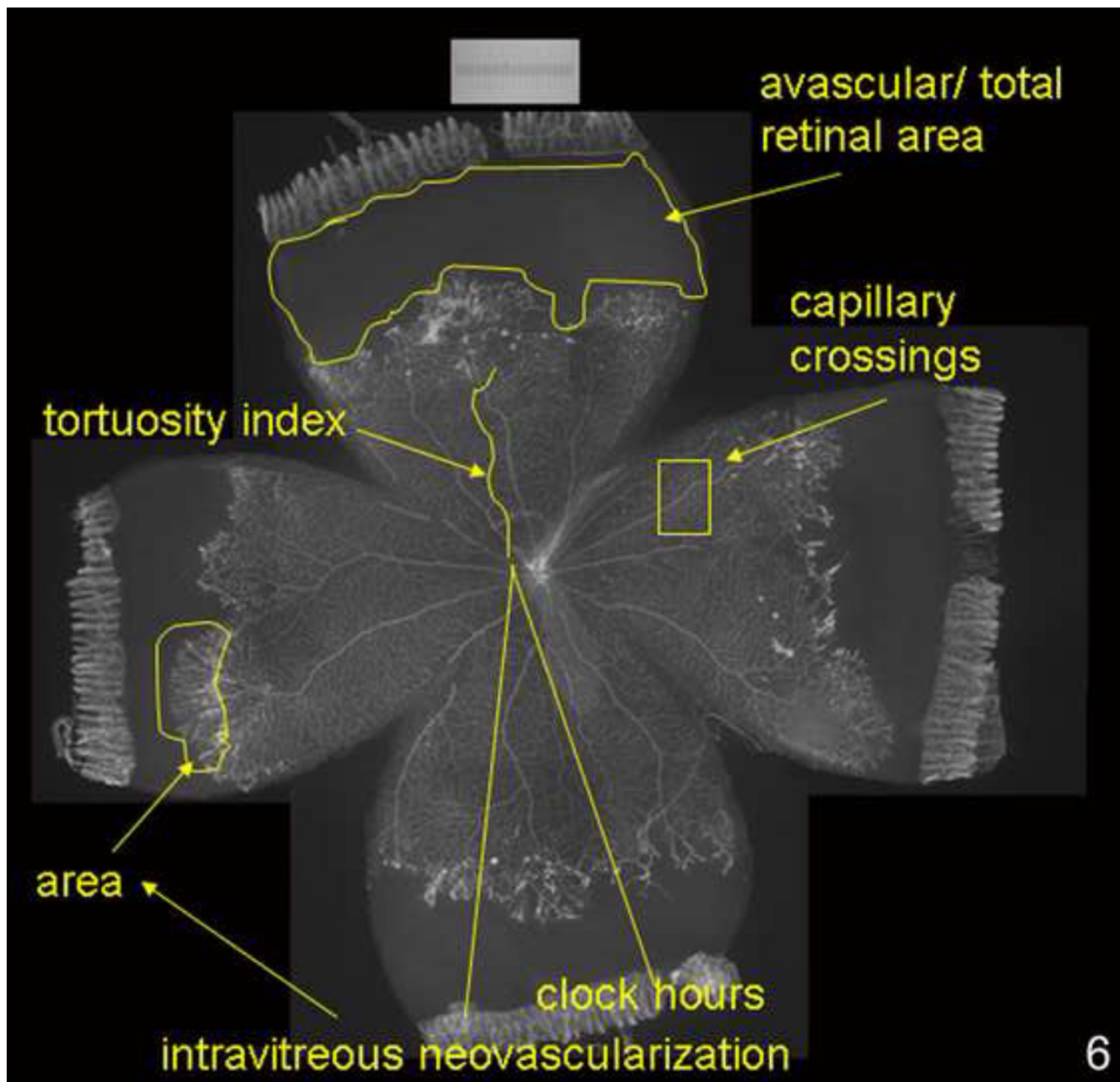
B. At p18, after return to room air for 4 additional days, intravitreal neovascularization develops at the junction of vascular and peripheral avascular retina.



**Figure 4.**  
 (top). Lectin-stained retinal flat mount of mouse model of hyperoxia induced vaso-obliteration and angiogenesis at p17 following 5 days of 75% oxygen and 5 days of room air showing central obliteration of retinal capillaries with endothelial budding (model developed by Lois Smith).  
 (bottom). Lectin-stained retinal flat mount of rat 50/10 model of oxygen induced retinopathy following 7 cycles of oxygen between 50% and 10%, then 4 days of room air exposure, showing peripheral avascular retina and intravitreal neovascularization at the junction of vascular and avascular retina.

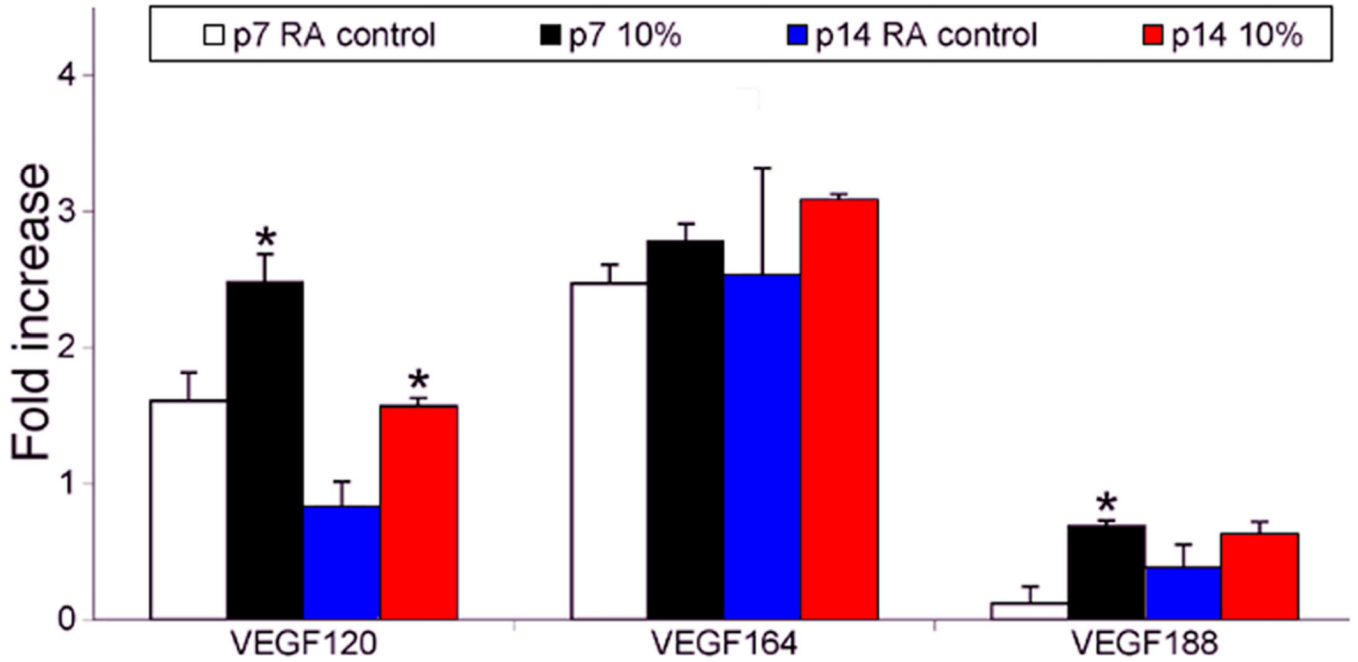


**Figure 5.** Graph of inspired oxygen over time in the 50/10 OIR developed by John Penn and 50/10 OIR+SO models. At postnatal day 14 pups are returned to room air (50/10 OIR) or recovered in supplemental oxygen (28% oxygen, 50/10 OIR+SO) models. The models have relevance to human ROP in that the arterial oxygen of pups in these oxygen extremes mimic the transcutaneous oxygen extremes in human preterm infants that develop severe ROP. Also fluctuations in oxygen are risks for ROP. The model also develops features similar to infants with severe ROP of today.



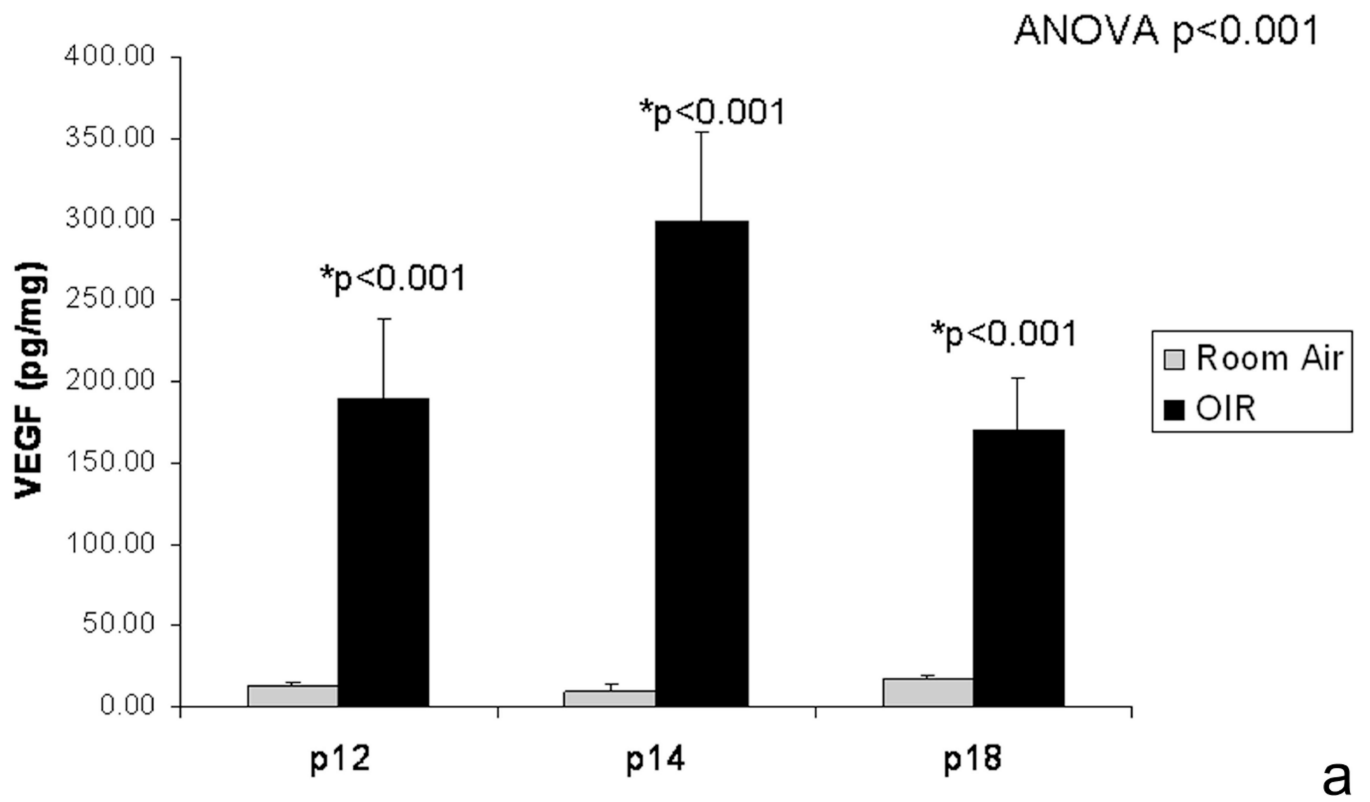
**Figure 6.**

Lectin-stained retinal flat mount of pup in 50/10 OIR model at postnatal day (p)18 after 7 cycles of oxygen fluctuations between 50% and 10% inspired oxygen and return to room air for 4 additional days showing what features can be quantified reproducibly in the model (avascular/total retinal area, clock hours or area of intravitreal neovascularization, tortuosity of retinal vessels, capillary density within vascularized retina).

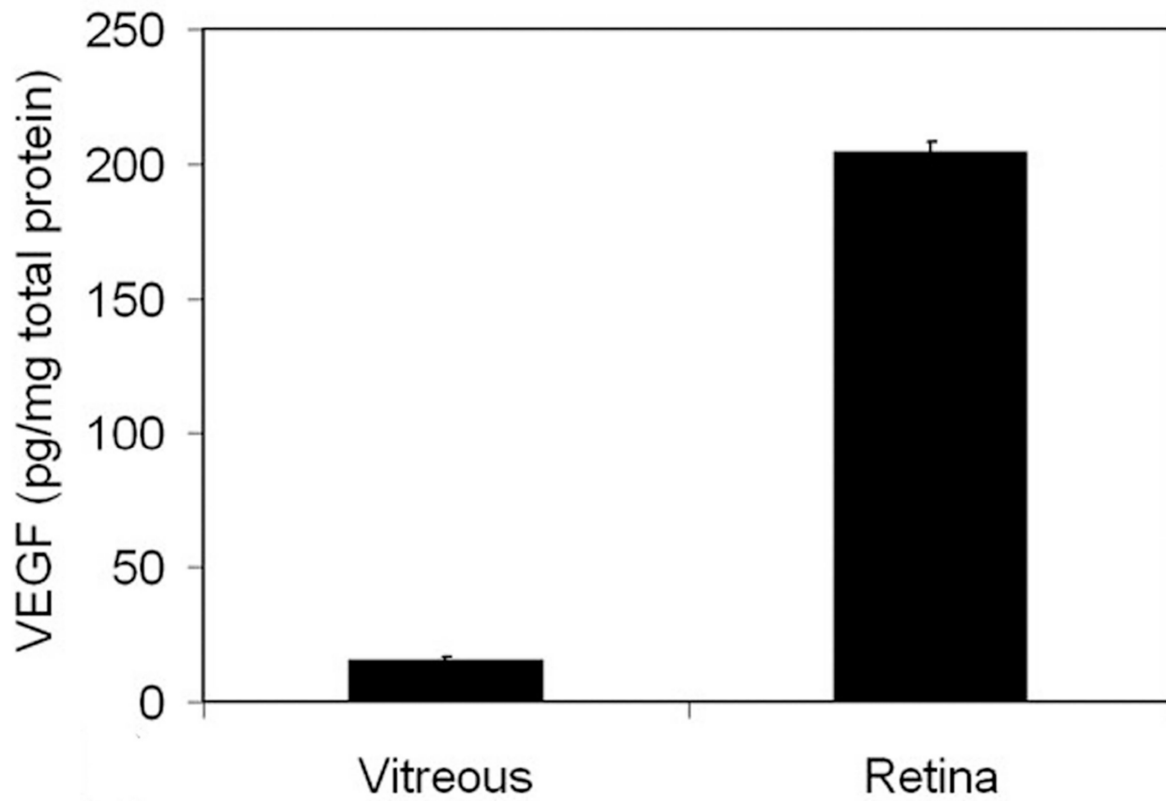


**Figure 7.**

Effect of a single episode of hypoxia on VEGF isoform expression. **A:** RT-PCR of VEGF isoform mRNAs in P7 (lane 1) and P14 (lane 3) control animals in room air (RA), and animals that had a single hypoxic episode of 24 h of 10% oxygen (10% O<sub>2</sub>) at either P7 (lane 2) or P14 (lane 4). PCR was repeated three times on different experiments and this result is representative. **B:** Densitometry measurements using 18S RNA as the control gene. Samples were assayed in triplicate and error bars are standard deviations. An asterisk (“\*”) indicates  $p < 0.01$  compared to respective controls, t test. (permission from *Molecular Vision* 2004; 10:512–20, <http://www.molvis.org/molvis/v10/a63>).







b

**Figure 8.**

- a. VEGF retinal protein from room air raised and 50/10 OIR exposed pups at different postnatal day ages by ELISA and showing increase in VEGF in retinas prior to development of intravitreal neovascularization and compared to room air
- b. At p18, retinal VEGF was 10-fold that in the vitreous. (permission from *Molecular Vision* 2008; 14:345–357, <http://www.molvis.org/molvis/v14/a43>).

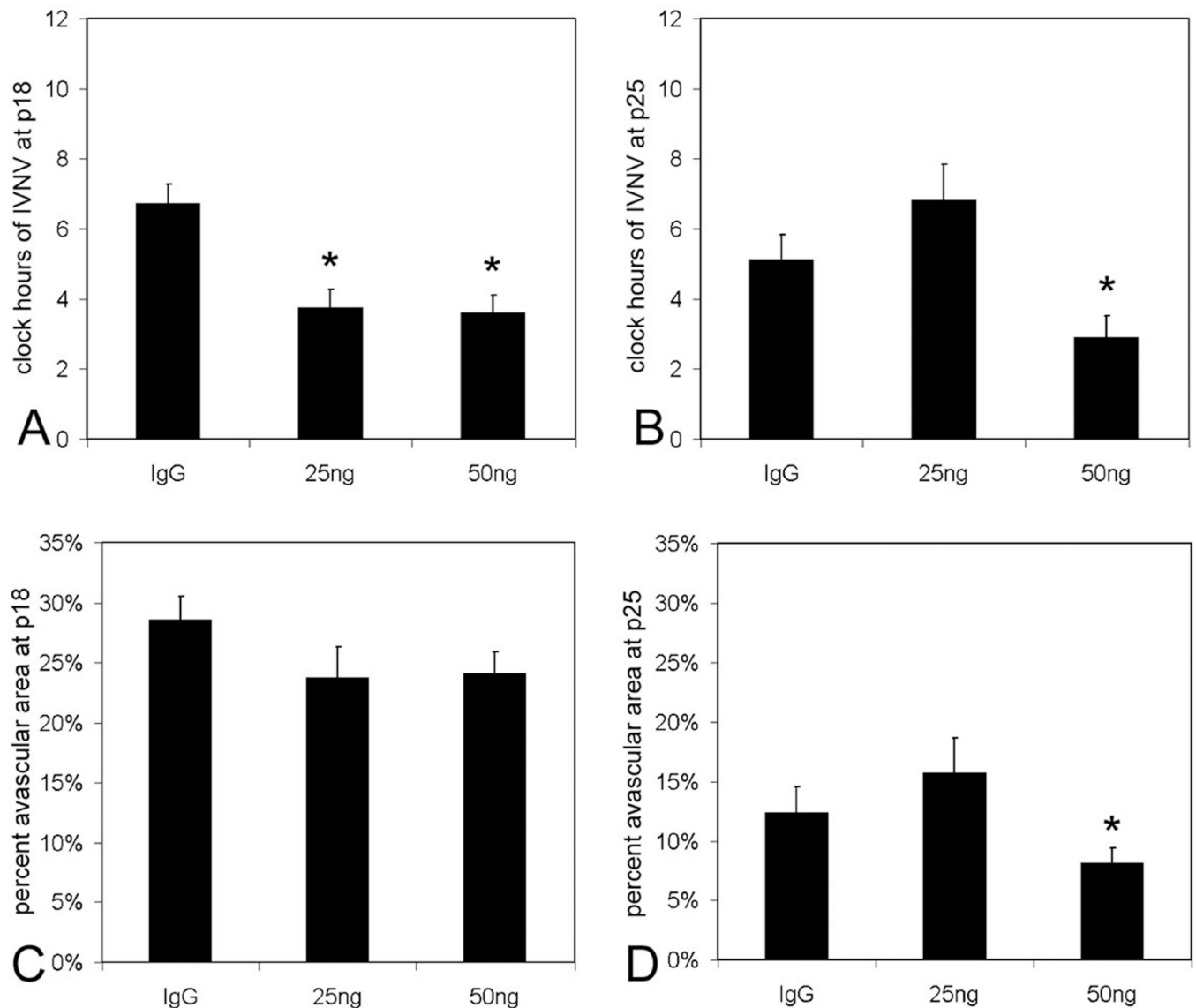


**Figure 9.**

Clock hours of intravitreal neovascularization and avascular/total retinal areas of lectin-stained retinal flat mounts from rat pups in 50/10 oxygen induced retinopathy after intravitreal injection of neutralizing antibody to vascular endothelial growth factor (VEGFab) or control nonimmune rat IgG. A: Mean clock hours of intravitreal neovascularization (IVNV) at p18 were significantly decreased by injection of either 25 ng or 50 ng VEGFab compared to IgG control (ANOVA  $p < 0.001$ ; \* posthoc Student's  $t$ -tests  $p < 0.001$  compared to IgG). B: Mean clock hours of IVNV at p25 were significantly decreased by injection of 50 ng VEGFab compared to IgG control (ANOVA  $p = 0.003$ ; \* posthoc Student's  $t$ -test  $p = 0.003$ ). C: Peripheral avascular/total retinal area was no different in retinas treated with either VEGFab dose compared to IgG control at p18 (ANOVA  $p = 0.238$ ). D: At p25, the overall ANOVA for peripheral avascular/total retinal area was significant ( $p = 0.038$ ). Posthoc testing showed the 50 ng dose of VEGFab was significantly decreased compared to the 25 ng dose (\* posthoc Student's  $t$ -test, 25 ng versus 50 ng,  $p = 0.038$ ). However, neither dose of VEGFab was significantly different to control IgG.

(permission from *Molecular Vision* 2008; 14:345–357, <http://www.molvis.org/molvis/v14/a43>).

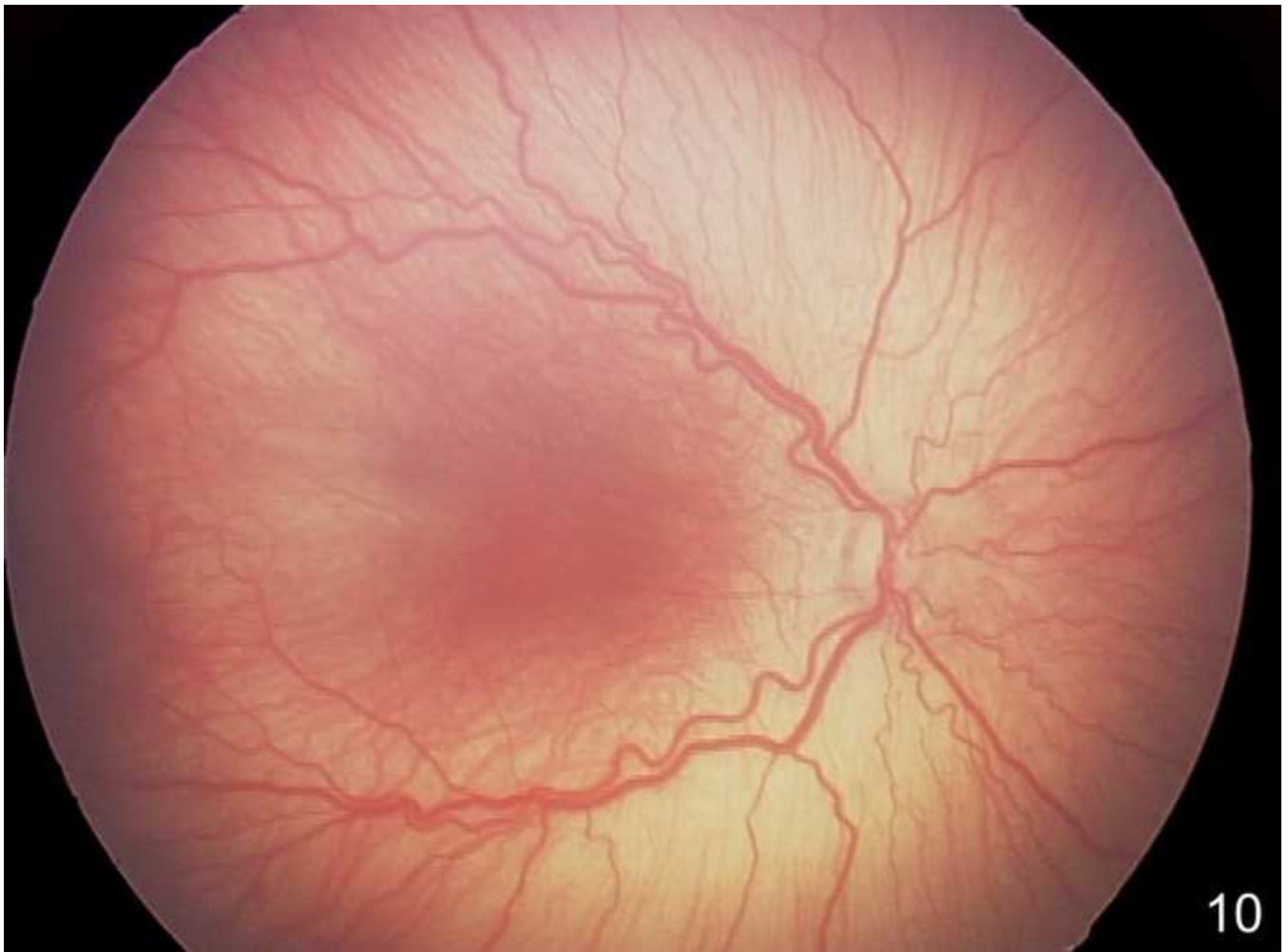


**Figure 10.** Retacam image (Clarity, CA) of right eye of human preterm infant demonstrating dilated and tortuous vessels seen in plus disease, a feature of severe ROP.

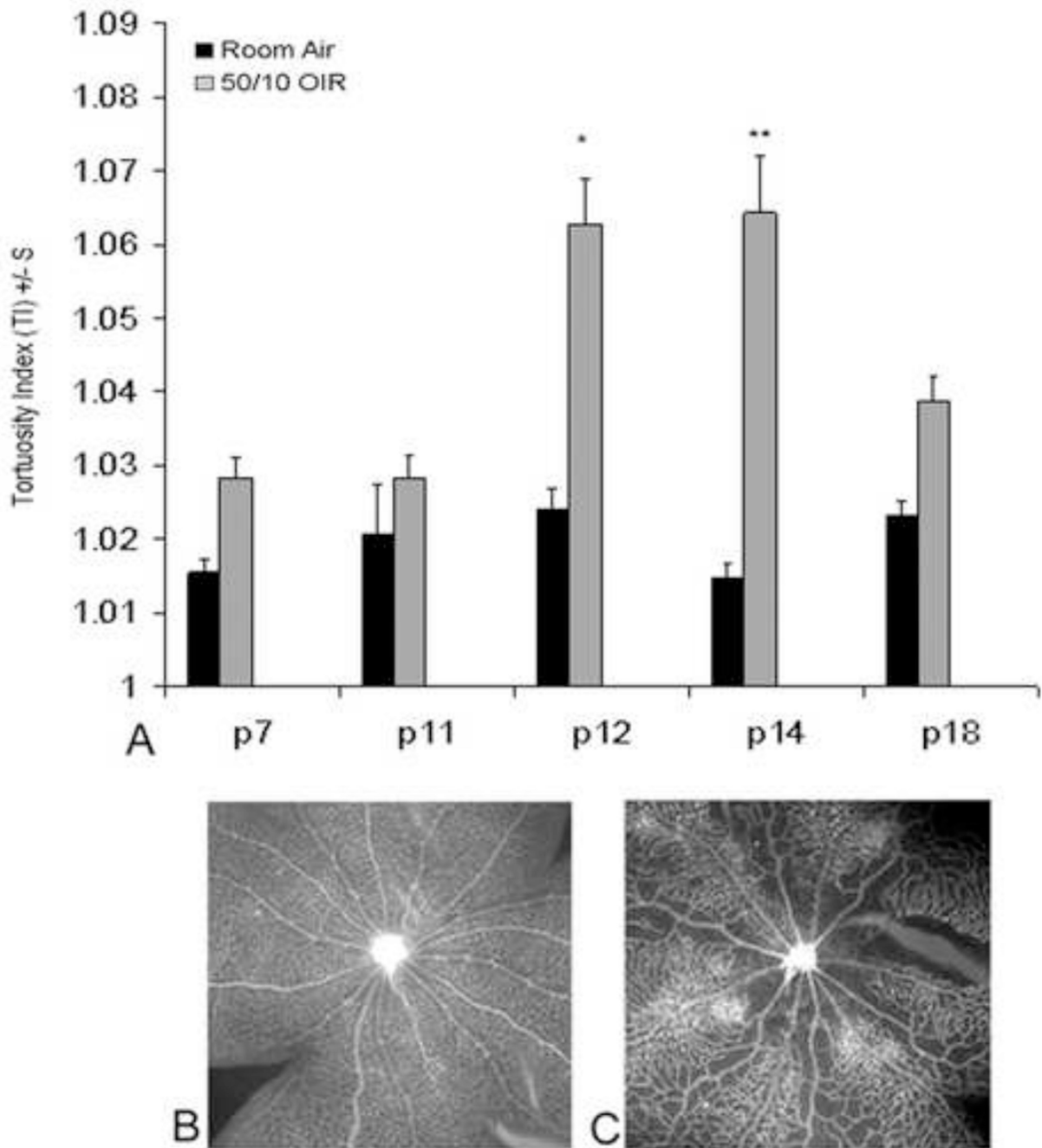


**Figure 11.**

A. Tortuosity indices in retinal arterioles measured in rats raised in room air or 50/10 OIR model at different postnatal day (p) ages showing increased tortuosity at p12 and p14.

Bottom: Representative lectin-stained retinal flat mount at p14 in room air (B) and 50/10 OIR (C) models. (re-plotted from *Investigative Ophthalmology and Visual Sciences*; 2008 Jul;49(7):3107–14).

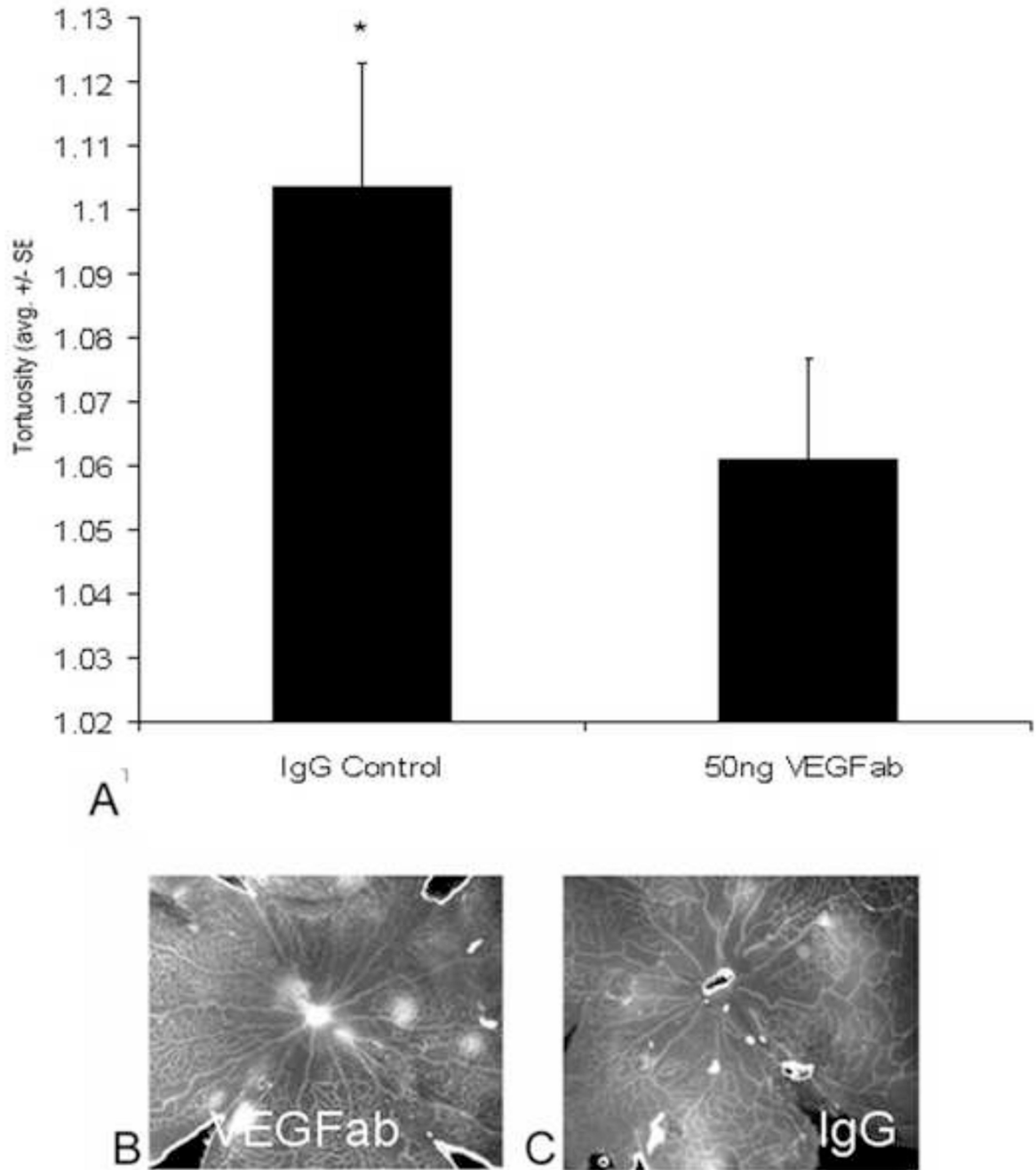


**Figure 12.**

Arteriolar tortuosity index of retinas from eyes injected with either 50 ng VEGF antibody (VEGFab) or 50 ng control IgG at p12 and analyzed at p14. (A) The tortuosity index was significantly reduced in eyes injected with 50 ng VEGFab compared with that in IgG-injected eyes (ANOVA  $*P = 0.004$ , post hoc protected  $t$ -test). (B) Examples of retinas from eyes injected with 50 ng VEGFab and (C) 50 ng control IgG resulted in tortuosity indices of  $1.03 \pm 0.007$  and  $1.11 \pm 0.04$ , respectively. (re-plotted from *Investigative Ophthalmology and Visual Sciences*; 2008 Jul;49(7):3107–14).

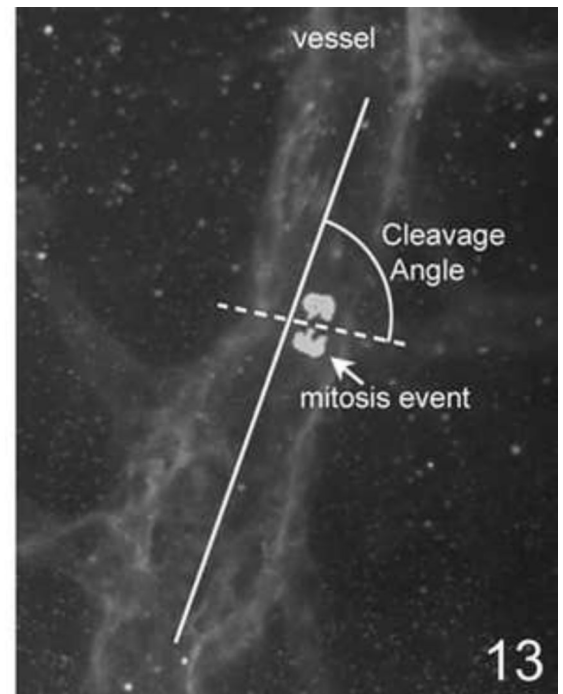
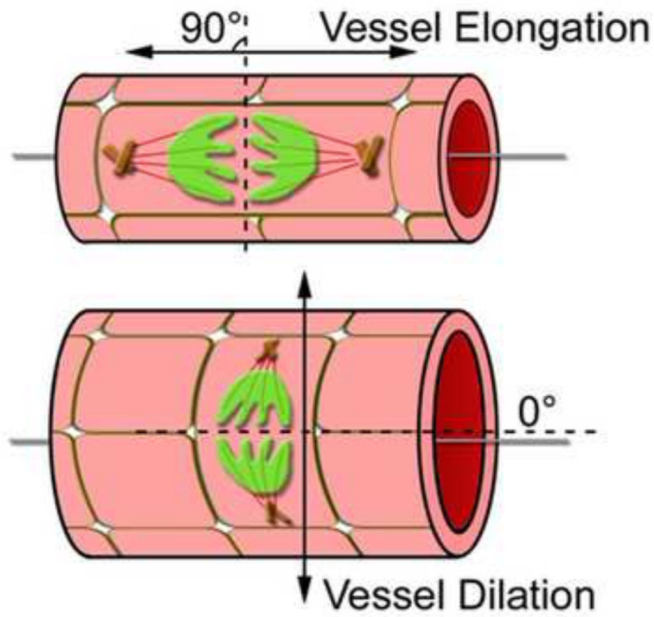


**Figure 13.**

Left: Artist diagram showing long axis of vessel and cleavage plane angle. An angle of 90 degrees predicts elongation of the vessel based on the migration of the dividing endothelial cells whereas an angle of 180 degrees predicts dilation. An irregular group of cleavage plane angles may be seen in disordered angiogenesis. Right: Lectin stained flat mounted vessel with cleavage planes drawn in to demonstrate how technique is performed.

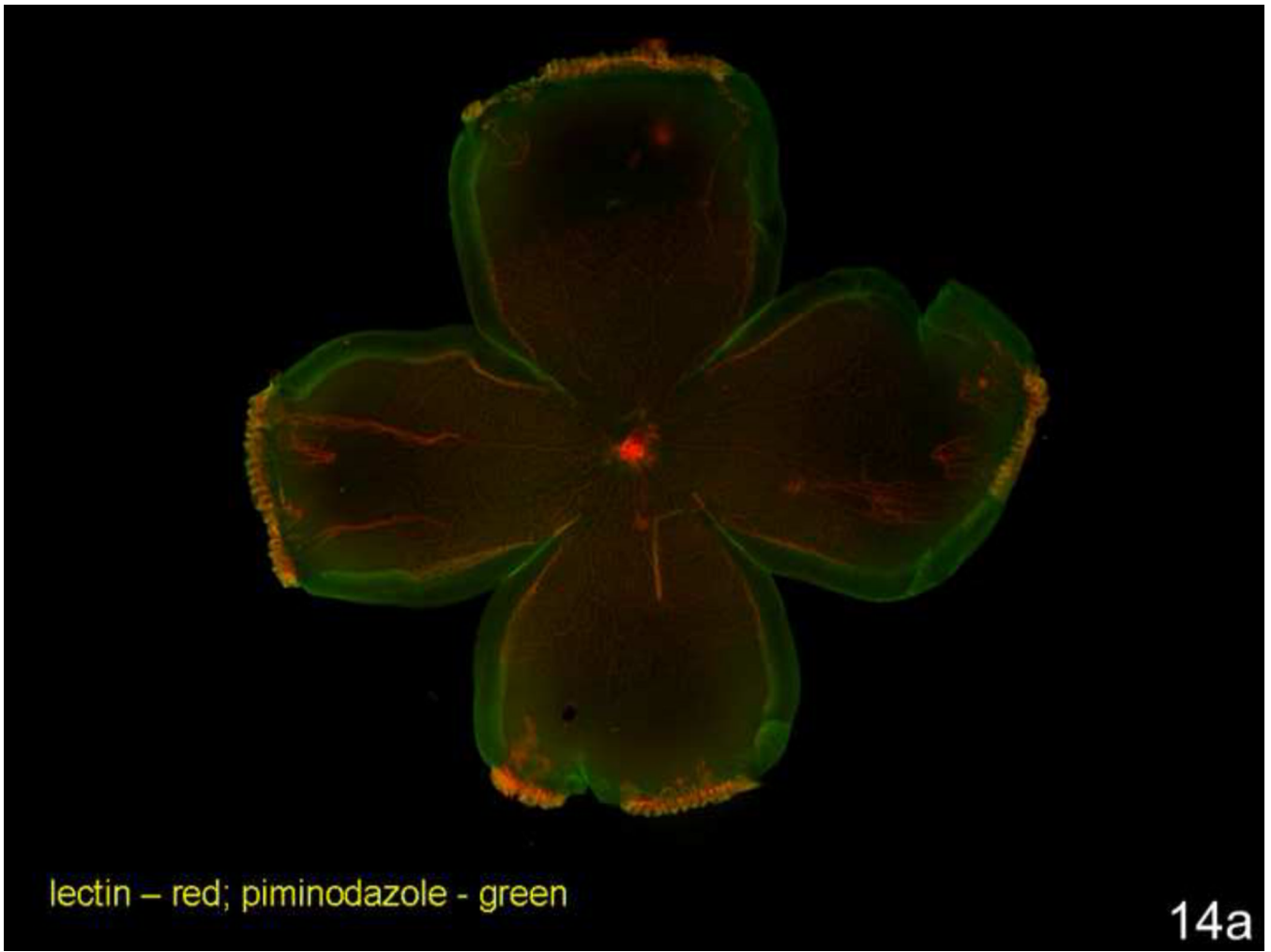
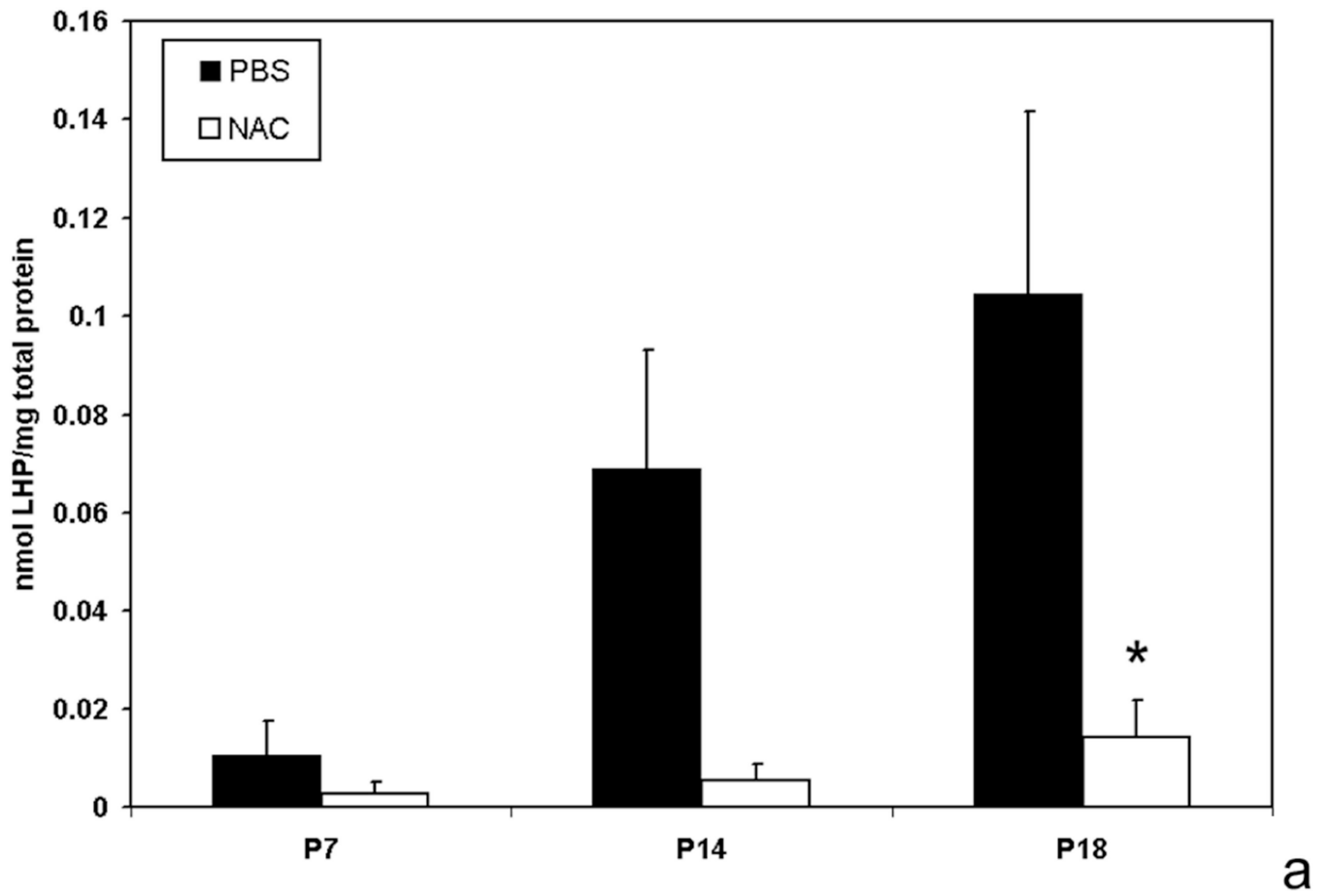


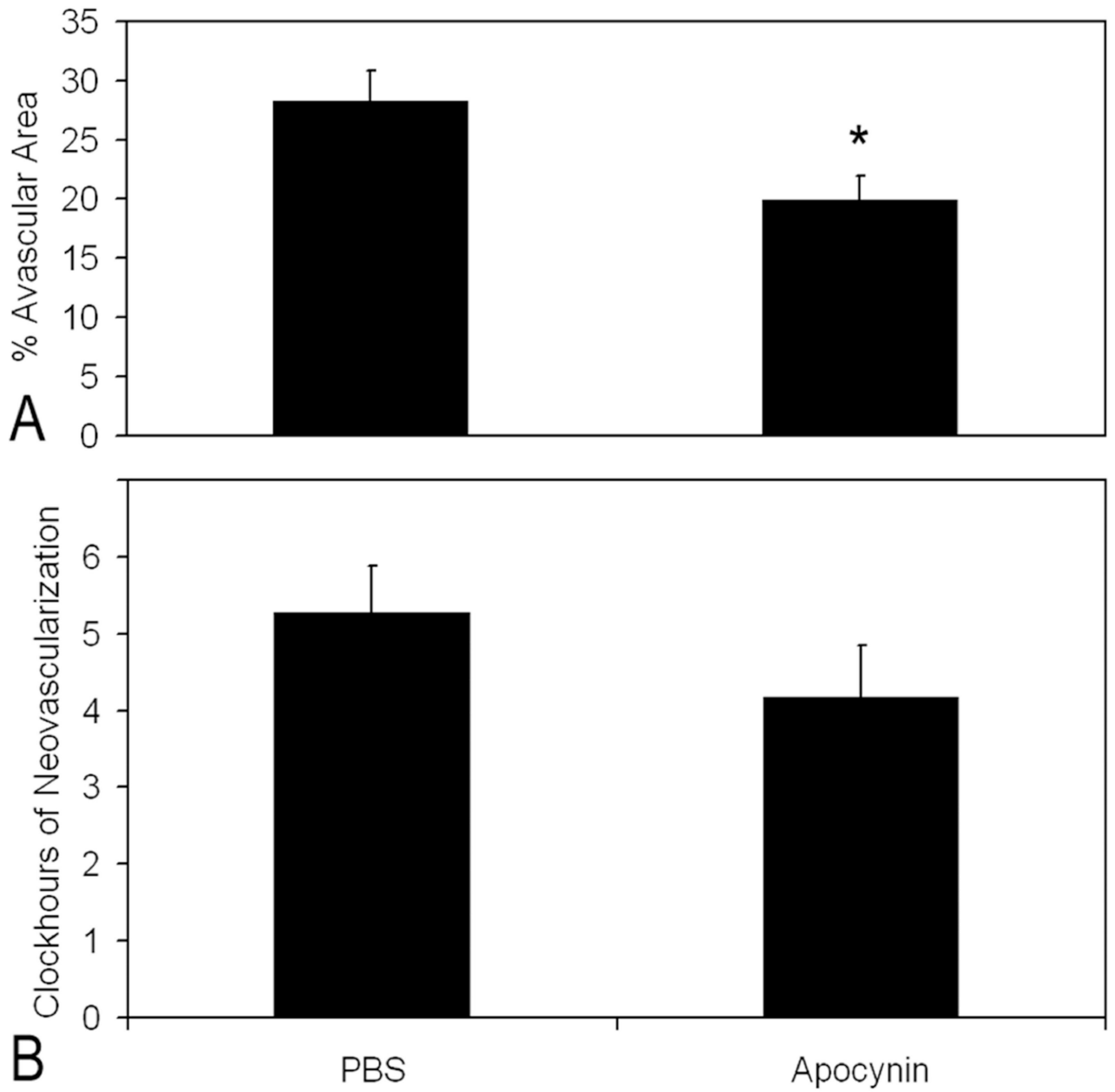




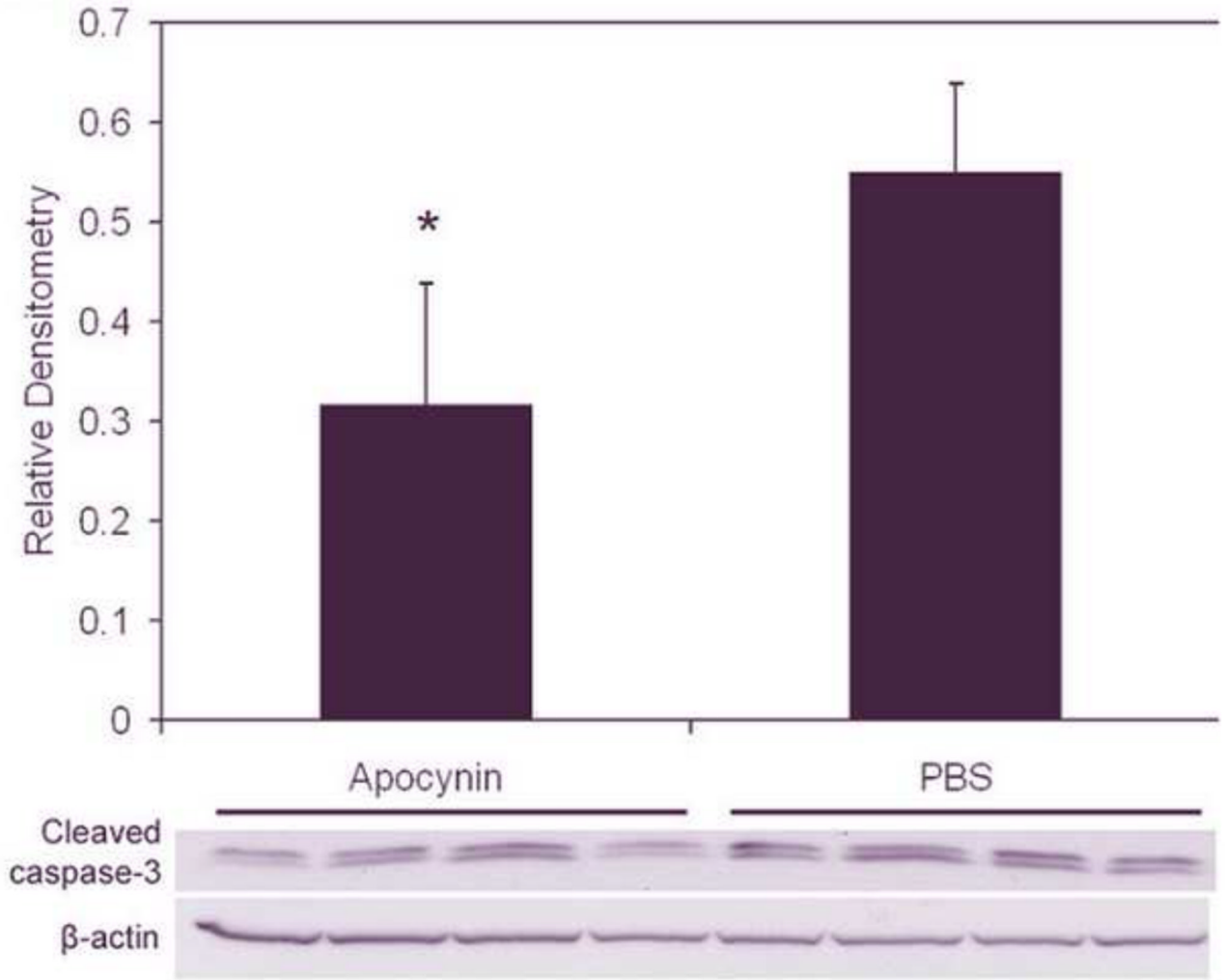
**Figure 14.**

- a. Lectin stained retinal flat mount of room air raised postnatal day (p)4 rat pup injected with pimonidazole 90 minutes before sacrifice. Lectin stains retina vessels (red) and insoluble pimonidazole conjugates (green) are present in tissue where oxygen concentration is less than 10 mm Hg. Despite nearly 50% of the retina as avascular, little insoluble pimonidazole is present.
- b. Lectin stained retinal flat mount of postnatal day (p)18 rat pup from the 50/10 OIR model injected with pimonidazole 90 minutes before sacrifice. Lectin stains retina vessels (red) and insoluble pimonidazole conjugates (green) are present in tissue where oxygen concentration is less than 10 mm Hg. Hypoxic retina (green labeling conjugated pimonidazole) is present in avascular retina and in areas in between vessels within vascularized retina.





b



C

**Figure 15.**

- a. Lipid hydroperoxide in 50/10 oxygen-induced retinopathy model. Lipid hydroperoxide (LHP) levels in retinas assayed at postnatal days 7, 14, or 18 (p7, p14, p18) from pups injected intraperitoneally (IP) with n-acetylcysteine (NAC) or PBS at postnatal days p2, p6, and p10 in the 50/10 oxygen-induced retinopathy (OIR) model. Overall ANOVA,  $p < 0.001$ , \*  $p = 0.012$ , Bonferroni post-hoc analysis comparing p18 NAC to p18 PBS injected. (n=8 animals at p7 and 4 animals at p14 and p18).
- b. Apocynin treatment significantly reduced percent avascular retina at p18 compared to PBS control. Avascular retinal area and clock hours of intravitreal neovascularization and capillary densities of apocynin treated pups. **A:** Percent avascular retinal area in 50/10 OIR model after intraperitoneal (IP) injections with apocynin once every 24 h from p12 to p17 and assayed at p18 was significantly reduced compared to phosphate buffered saline (PBS) injected pups (\*  $p = 0.017$ , Student's t-test; n=11 retinas each). **B:** Clock hours of intravitreal neovascularization (IVNV) in retinas from 50/10 OIR model after IP injections with apocynin once every 24 h from p12 to p17 and assayed at p18 were not significantly different to PBS injected pups ( $p = 0.26$ ; Mann-Whitney test, n=11).

c. Cleaved caspase-3 expression in the retinas of 50/10 OIR after IP injection with apocynin on p12 and p13 and assayed on p14 was significantly decreased compared to retinas from PBS injected pups ( $p=0.021$ , Student's t-test,  $n=4$ ). However, no significant difference in cleaved caspase-3 expression was measured in retinas of pups injected with apocynin every 24 h from p12 to 17 and assayed on p18 compared to PBS injected pups ( $p=0.78$ , Student t-test, data not shown). (permission from *Molecular Vision* 2007; 13:840–53 <http://www.molvis.org/molvis/v13/a92/>)

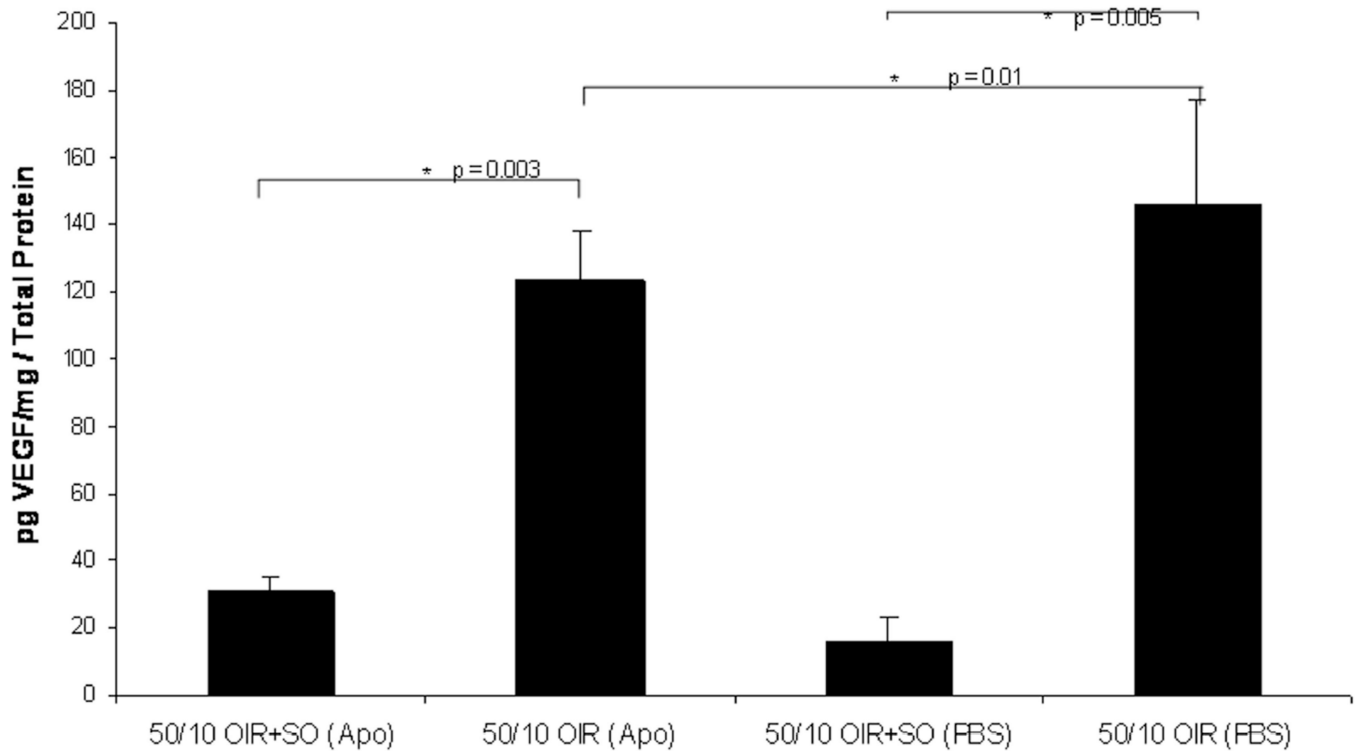
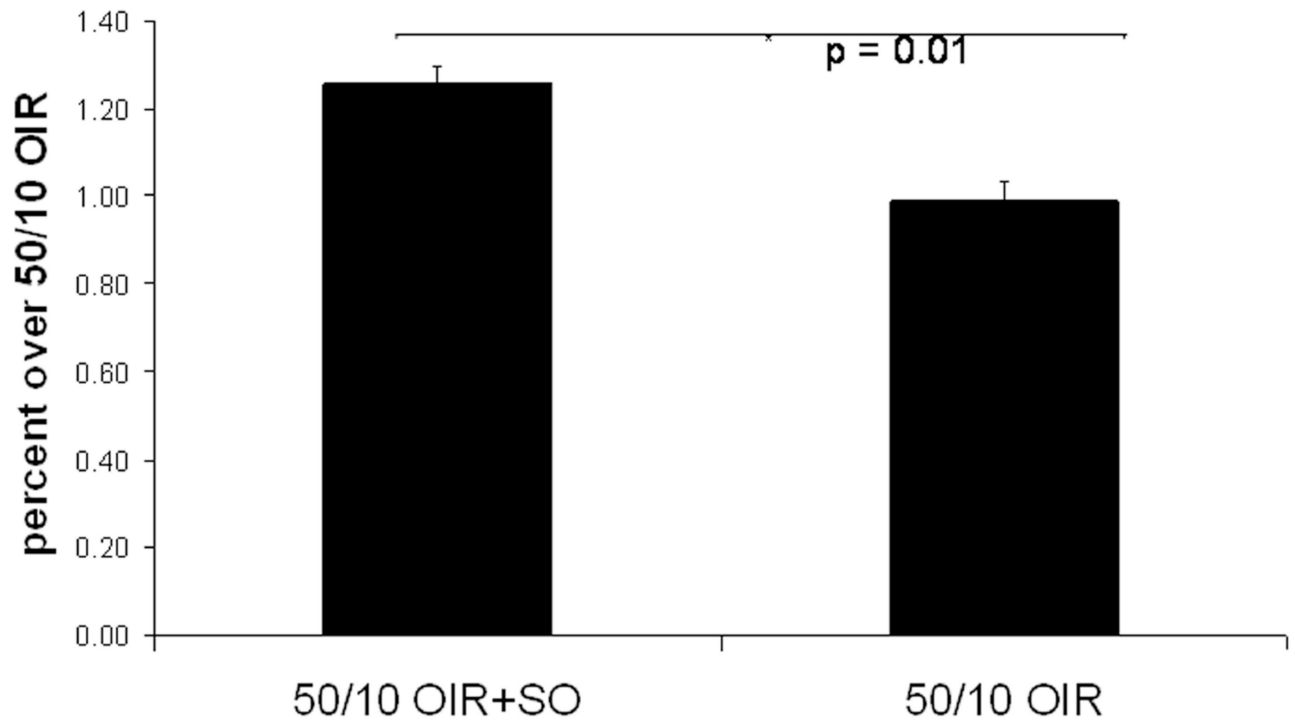
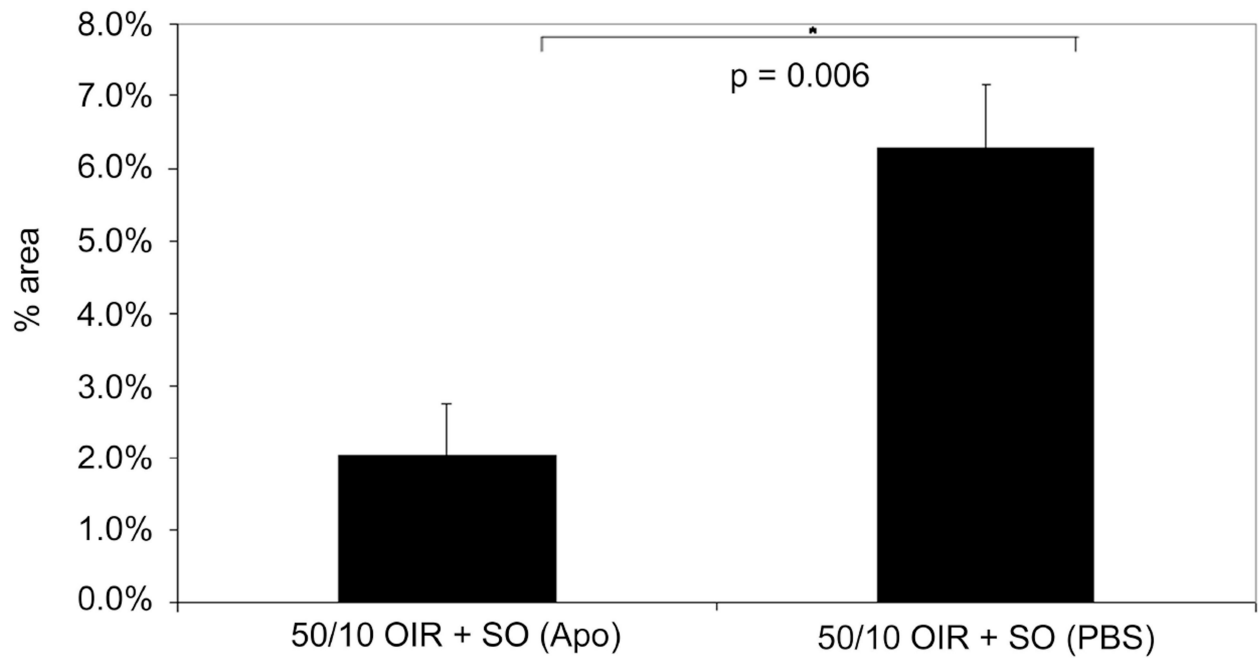


**Figure 16.** ELISA of VEGF from pups in 50/10 OIR or in 50/10 OIR+SO models treated with either IP injections of apocynin (10mg/kg/day) or equivalent volume of PBS from p12-p17 and assayed at p18. Student's t-test. (re-plotted from *Investigative Ophthalmology and Visual Sciences*, 2008; 49(4);1591–1598.)



a



b

**Figure 17.**

a. Phosphorylated p47-phox, a subunit of activated NADPH oxidase, is increased in the 50/10 OIR+SO model compared to 50/10 OIR model.

b. Inhibition of ROS from activated NADPH oxidase using apocynin reduces area of intravitreal neovascularization in the 50/10 OIR+SO model. (re-plotted from *Investigative Ophthalmology and Visual Sciences*, 2008; 49(4);1591–1598.)



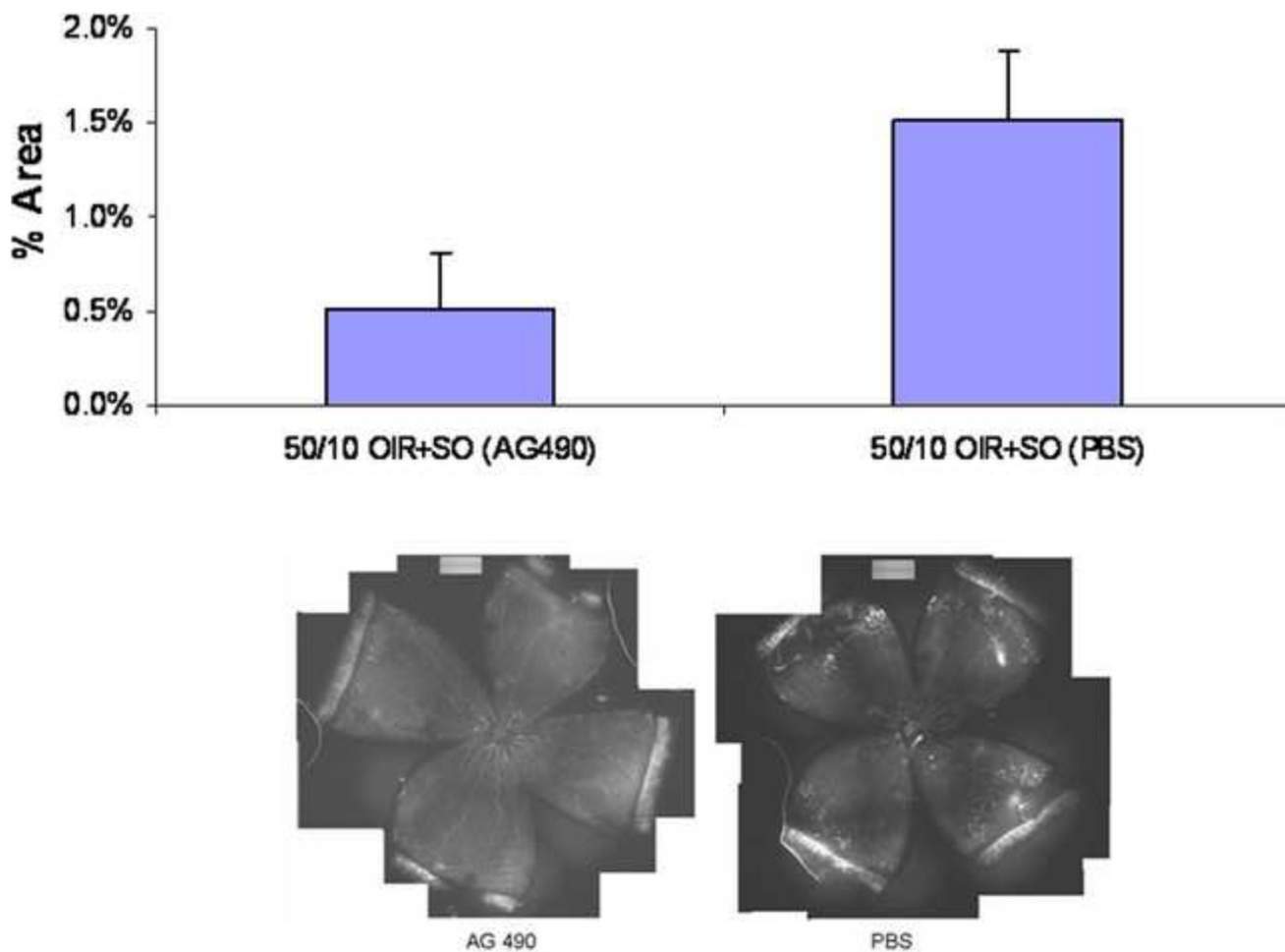


**Figure 18.**

Areas of intravitreal neovascularization (IVNV) at postnatal day (p)18 in retinas from the 50/10 OIR+SO model treated with daily intraperitoneal (IP) injections (5mg/kg) of AG490 or PBS starting at p3 and continuing through p17. Top: Mean pixel density in 10 or more retinas analyzed per group, \* $p=0.03$ . Bottom: Flat mount image representative of each treatment group. (re-plotted from Investigative Ophthalmology and Visual Sciences, 2009; in press.)

**Table 1**

Avascular/total Retinal Area and Intravitreal Neovascularization at Different Postnatal Day Ages in Room Air and 50/10 OIR Raised Rats

| Postnatal day age (p) | Avascular/total retinal area % (RA) | Avascular/total retinal area % (50/10 OIR) | Clock hours of IVNV (RA) | Clock hours of IVNV (50/10 OIR) |
|-----------------------|-------------------------------------|--|--------------------------|---------------------------------|
| 2*                    | 61.1                                | 82.8                                       | 0                        | 0                               |
| 7**                   | 24.3                                | 51.2                                       | 0                        | 0                               |
| 14                    | 0                                   | 32.8                                       | 0                        | 0                               |
| 18                    | 0                                   | 23.1                                       | 0                        | 9.5                             |

p2 - one 24 hour period of 50% oxygen followed by a 24 hour period of 10% oxygen and processed following the 10% oxygen cycle.

p7 - cycles repeated between 24 hours of 50% oxygen and 24 hours of 10% oxygen until day 7; analysis performed followed 50% oxygen (reformatted from data from *Molecular Vision* 2004; 10:512–20, <http://www.molvis.org/molvis/v10/a63>).

**Table 2**

VEGF protein values in 50/10 OIR model and room air (ELISA pg/mg protein)

| ELISA VEGF               | P0    | P8    | P11  | P12   | P13   | P14   | P18   |
|--------------------------|-------|-------|------|-------|-------|-------|-------|
| 50/10 OIR                | 19.64 | 408.9 | 35.5 | 195.0 | 571.4 | 393.2 | 296.9 |
| RA                       | 19.6  | 34.9  | 58.0 | 51.5  | 23.8  | 40.2  | 43.8  |
| Ratio of 50/10 OIR to RA | 1.0   | 11.7  | 0.6  | 3.8   | 24    | 9.8   | 6.8   |

**Table 3**

Retinal or Vitreous VEGF protein levels in rats in 50/10 OIR model or room air

|           | <b>Retinal VEGF<br/>p12</b> | <b>Retinal VEGF<br/>p14</b> | <b>Retinal VEGF<br/>p18</b> | <b>Vitreous VEGF<br/>p18</b> |
|-----------|-----------------------------|-----------------------------|-----------------------------|------------------------------|
| Room Air  | 12.22 (2.4)                 | 9.6 (4.3)                   | 16.87 (2.7)                 | 16 (1.0)                     |
| 50/10 OIR | 189.65 (49.7)               | 298.55 (55.9)               | 169.94 (32.5)               | 190 (23)                     |

Values are in pg/mL. () – indicate standard errors.